IMPLICATIONS FOR THERMAL HISTORIES OF THE SAN JUAN BASIN AND SAN JUAN MOUNTAINS SINCE LATE CRETACEOUS TIME

by

Gerry W. Clarkson

Dr. Carn
Thanks, b
wishes!
Gerry

Submitted in Partial Fulfillment of
the Requirements for the Degree of
Doctor of Philosophy

NEW MEXICO INSTITUTE OF MINING AND TECHNOLOGY

Socorro, New Mexico

May 1984

TABLE OF CONTENTS

ACKNOWLEDGEMENTS

I thank my advisor, Dr. Marshall Reiter, whose inspiration, guidance and encouragement made the successful completion of this work possible. I also thank the other members of the advisory committee: Dr. Kent Condie, Dr. Alan Gutjahr, Dr. Allan Sanford, and Dr. John Schlue. I am also grateful to my wife, Marie, for her support and encouragement.

I gratefully acknowledge the financial support of the New Mexico Bureau of Mines and Mineral Resources. I also thank the Geoscience Department and the Computer Center of the New Mexico Institute of Mining and Technology for their aid.

LIST OF FIGURES

LIST OF TABLES

ABSTRACT

The observed heat flow in the San Juan Basin and San Juan volcanic field, and the maturation level of the Fruitland Formation coals across the San Juan Basin are used to constrain thermal history models of the San Juan Basin. The heat flow and coal maturation level across the Basin appear to have been influenced by a thermal source associated with the San Juan volcanic field. Time-dependent isothermal step models suggest that the observed heat flow may be best modelled by a steady-state isothermal step extending from 30 to 98 km depth whose edge underlies the northern San Juan Basin. The maturation levels of the Fruitland coals across the Basin are not inconsistent with a steady-state model; however, the observed maturation levels in the northern and central San Juan Basin require more heat than can be associated with conduction away from the deep thermal source (steady-state step) and from the shallow crustal batholith which underlies the San Juan volcanic field. The magmatic activity or burial depths which would be required to explain the observed maturation levels in the northern and central Basin are inconsistent with the geologic history of the San Juan Basin. It appears that heat advection by ground-water movement has influenced the coal maturation levels in the Basin. The ground water may have been heated by both shallow magmatic activity

associated with the emplacement of the San Juan batholith and elevated geothermal gradients associated with the steady state thermal source. An appreciation of heat advection by ground-water movement is important to understanding regional patterns of heat flow and hydrocarbon maturation.

INTRODUCTION

The Late Cretaceous and Cenozoic geologic history of the San Juan Basin and the neighboring San Juan Mountains (Figure 1) depends upon the thermal processes transferring heat into and within the earth's crust. The San Juan Mountains region has experienced Laramide, Oligocene and Miocene magmatic activity (Lipman et al, 1978; Tweto, 1975; Dickinson et al, 1968). The observed heat flow in the San Juan Basin increases as the San Juan volcanic field is approached, suggesting a large thermal source associated with the San Juan volcanic field (Reiter and Mansure, 1983; Reiter and Clarkson, 1983a). The regional pattern of coal maturation and petroleum occurrence in the San Juan Basin also suggests that a large thermal source has been influential in at least the northern part of the San Juan Basin (Reiter and Clarkson, 1983b; Rice, 1983).

Reiter and Clarkson (1983a) note that the observed heat flow in the northern San Juan Basin requires a thermal source whose dimensions are larger than those of the San Juan batholith. They demonstrate that the observed heat flow cannot be associated only with a column of magma which has been cooling since the end of the Oligocene activity, that is to say that the thermal source is in some sense replenished. Reiter and Clarkson (1983b) and Rice (1983) have suggested that the coal maturation in the San Juan

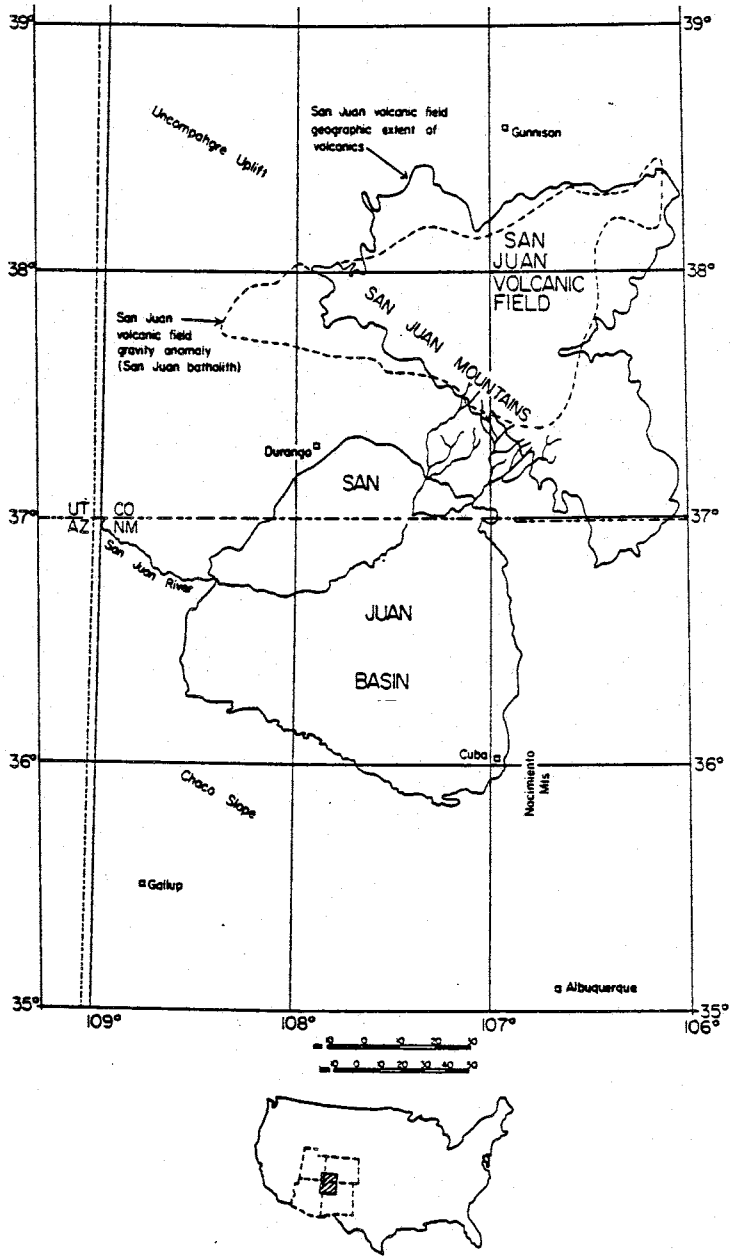

Figure 1. San Juan region, northwestern New Mexico and southwestern Colorado. Edge of the San Juan batholith defined from gravity data (Plouff and Pakiser, 1972).

Basin requires additional heat from a thermal source associated with the San Juan batholith. The extent of influence of a thermal source is determined in part by the nature of the source, for example its size, shape, depth, and heat content. The extent of influence will also be determined by the manner in which heat is transferred from the source into the surrounding region. For example, if water movement transfers heat away from the source the region of influence may be greater than if heat is transferred only by conduction.

This study investigates the San Juan thermal source and its heating effects in the San Juan Basin. A knowledge of the thermal source should give some insight into the tectonic and magmatic processes which have occurred in the San Juan region. The size, location and amount of heat contained in the thermal source are important parameters in defining the origin of the source and the relationship between the source and the geology of the area. For example the present day heat-flow profile across the San Juan Basin suggests a deep (mantle) heat source replenished since Oligocene time (Reiter and Clarkson, 1983a). A steady-state thermal model suggests a source whose edge is near the boundary of differential uplift in the northern San Juan Basin (Reiter and Clarkson, 1983a).

In order to investigate the San Juan thermal source and its heating effects across the San Juan Basin, both heat flow and coal maturation data are employed. Heat-flow data indicate the present near surface thermal regime of the area. Maturation data indicate the total amount of heating of the coal since its deposition. In this study finite-difference numerical techniques were used to investigate time-dependent thermal models of the San Juan region. Temperature variations with time, needed to estimate the coal maturation across the San Juan Basin, were obtained using time-dependent thermal models subjected to the constraint that heat-flow values predicted by the model be compatible with the present observed heat flow. Compatibility between calculated and observed coal maturation values was used to constrain models of the burial depth of the coals through time in the San Juan Basin and the heating effects of the San Juan thermal source.

LATE CRETACEOUS AND TERTIARY GEOLOGY OF THE SAN JUAN REGION

San Juan Basin

The San Juan Basin is a large sedimentary basin located in the southeastern part of the Colorado Plateau (Figure 1). Basin subsidence began during Laramide time, accelerated in the Early Tertiary, and ceased by the Late Paleocene or Early Eocene (Tweto, 1975; Stone et al, 1983). The maximum structural relief noted in the Basin is about 3 km along the San Juan uplift (Kelly, 1950).

In Late Cretaceous time five transgression-regression cycles of the Western Interior seaway occurred across the region (Molenaar, 1983). During the final regression of the seaway the marine Pictured Cliffs Sandstone and the nonmarine Fruitland Formation and Kirtland Shale were deposited. The Fruitland Formation, which contains the principle coal reserves of the San Juan Basin, is composed of coastal swamp, river, flood plain and lake deposits (Fassett and Hinds, 1971). After deposition of the Kirtland Shale, the Late Cretaceous in the San Juan Basin was a time of erosion, with perhaps as much as 0.6 km of Late Cretaceous deposits being removed in the southeastern part of the Basin (Fassett and Hinds, 1971).

As Basin subsidence continued in Early Tertiary time, stream channel deposits were laid down. These deposits include the Ojo Alamo Sandstone, Nacimiento Formation, and Animas Formation of Paleocene age and the San Jose Formation of Eocene age (Baltz, 1967; Fassett and Hinds, 1971). The Animas Formation contains large amounts of volcanic debris derived from the highlands to the north and northeast of the Basin (Baltz, 1967). The time following deposition of the San Jose Formation has been one of nondeposition and/or erosion in the Basin (Baltz, 1967). Stone et al (1983) estimate that perhaps as much as 0.3 km of the San Jose Formation may have been eroded in the central part of the San Juan Basin.

San Juan Mountains

The San Juan Mountains have experienced recurrent tectonic and magmatic activity. The region was part of the Late Paleozoic Uncompahgre-San Luis highland which was rejuvenated in Laramide time (Tweto, 1975). The San Juan Mountains are an Oligocene volcanic feature resting in part on the Needle Mountains, an exposed Laramide domal uplift, and in part on the truncated San Luis-Uncompahgre uplift (Steven, 1975; Tweto, 1975).

Immediately prior to the Laramide orogeny the region of the present San Juan Mountains was a flat, slowly subsiding marine enviroment (Dickinson et al, 1968; Tweto, 1975). During the Laramide orogeny the region was uplifted, folded, faulted, and intruded (Dickinson et al, 1968; Tweto, 1975). Tweto (1975) indicates that the Laramide orogeny in this region began in the Late Cretaceous (~72 mya) and continued into the Eocene. Igneous activity began about 70 mya, peaked early in the Laramide and ceased about 63 mya (Tweto, 1975). The Cretaceous-Early Tertiary igneous activity may be associated with the emplacement of Laramide batholiths in the San Juan region (Tweto, 1975).

During Eocene time erosion reduced the Laramide uplifts to a low plain (Steven, 1975). In Oligocene time 60,000 km^3 of volcanic material was erupted, the remnant of which is the present San Juan volcanic field (Lipman et al, 1978). The Oligocene volcanism occurred in two phases: the first phase of volcanism, which accounts for 2/3 of the volcanic material, occurred about 35-30 mya and the second phase of volcanism occurred about 30-26.5 mya (Lipman et al, 1978). The first phase consisted of intermediate composition magmas which are thought to have equilibrated in the lower crust or the mantle while the magmas of the second phase were more silicic and are thought to have equilibrated in the upper crust (Lipman et al, 1978). It has been suggested that both phases are associated with the rise and emplacement of a large upper crustal batholith (Steven, 1975; Lipman et al,

1978). Lipman et al (1978) suggest that the magmas were ultimately derived from the mantle and may have been associated with subduction processes.

In Miocene and Pliocene times the San Juan Mountains were within an extensional enviroment. During this time bimodal basalt-rhyolite volcanic rocks were erupted (Lipman et al, 1978). Lipman et al (1978) suggest the basaltic magmas originated in the mantle; and, as the basaltic magmas rose, they provided the heat energy necessary to produce the crustal rhyolitic magmas. The Miocene-Pliocene volcanism appears to be genetically unrelated to the Oligocene volcanism (Lipman et at, 1978).

MODELLING OF THE SAN JUAN REGION THERMAL HISTORY

Coal Maturation and Heat-Flow Data

Observed heat flow and level of coal maturation are the two parameters used to model the thermal history of the San Juan region. The surface heat flow is related to the present-day thermal conditions in the area. Any thermal history proposed for the San Juan region is constrained by the observed heat flow, that is, any proposed thermal history must lead reasonably to the present thermal conditions in the region. The level of coal maturation is related to the temperature history of an area. Hydrocarbon maturation is thought to be basically a first order chemical reaction, linearly dependent on time and exponentially dependent on temperature (Lopatin and Bostick, 1974; Waples, 1980). Thus the level of coal maturation in the San Juan region will provide a constraint on the thermal history of the region.

Table 1 and Figure 2 present coal maturation data for the Fruitland coals from the San Juan Basin. The maturation data has been adapted from Fassett and Hinds (1971). The level of coal maturation is given in terms of percent vitrinite reflectance (R_o). Coal maturation values from Fassett and Hinds (1971) were given in terms of percent volatile matter. These data have been converted to

Table 1. Maturation level of the Fruitland Formation coals in the San Juan Basin (after Fassett and Hinds, 1971).

Well	North Latitude	West Longitude	% Vitrinite Reflectance (R_o)
1. El Paso Natural Gas Bondad 34-10 No. 3X	37° 09'	107° 53'	1.12
2. Mobil Oil Schofield Auto 31X-5	37° 03'	107° 38'	1.18
3. Atlantic Refining Southern Ute 32-10 No. 15-1	37° 01'	107° 55'	1.06
4. Delhi-Taylor Wickens No. 1	36° 58'	107° 49'	0.87
5. La Plata Gathering San Juan Unit 32-50 No. 2-27	36° 57'	107° 26'	1.11
6. El Paso Natural Gas Rosa Unit No. 41	36° 56'	107° 24'	0.99
7. Consolidated Oil and Gas Mitchell No. 1-5	36° 56'	108° 07'	0.53
8. El Paso Natural Gas Case No. 9	36° 55'	108° 01'	0.51
9. Consolidated Oil and Gas Freeman No. 1-11	36° 55'	108° 10'	0.50
10. Delhi-Taylor Barret No. 1	36° 53'	107° 48'	0.70
11. Delhi-Taylor Moore No. 6	36° 50'	107° 42'	0.57
12. Aztec Oil and Gas Ruby Jones No. 1	36° 50'	108° 02'	0.53
13. El Paso Natural Gas S.J.U. 30-6 No. 37	36° 49'	107° 27'	0.96

Table 1 (continued)

14. R and G Drilling Lunt No. 62	36° 49'	108° 15'	0.47
15. Southwest Production Sullivan No. 1	36° 48'	108° 04'	0.51
16. N.M.P.S.C.C. Core Hole No. 7	36° 48'	108° 23'	0.46
17. El Paso Natural Gas Turner No. 3	36° 47'	107° 47'	0.49
18. El Paso Natural Gas Ludwick No. 20	36° 47'	107° 55'	0.54 0.44
19. Compass Exploration Federal No. 1-31A	36° 47'	108° 15'	0.47
20. El Paso Natural Gas S.J.U. 29-5 No. 17	36° 45'	107° 23'	0.72
21. Aztec Oil and Gas Grenier "B" No. 3	36° 45'	107° 55'	0.45 0.51
22. El Paso Natural Gas S.J.U. 29-6 No. 66	36° 44'	107° 28'	0.72
23. Tidewater N.M.-Fed. No. 12-E	36° 44'	107° 57'	0.55
24. International Oil Fogelson No. 1-9	36° 44'	108° 00'	0.47
25. Tennesee Oil and Gas, Cornell Gas Unit A No. 1	36° 44'	108° 05'	0.47
26. Aztec Oil and Gas Cain No. 16-D	36° 42'	107° 49'	0.49
27. Aztec Oil and Gas Hagood No. 21-6	36° 42'	108° 14'	0.44
28. Aztec Oil and Gas Hagood No. 13-6	36° 41'	108° 10'	0.46
29. Humble Oil and Gas Humble No. L-9	36° 41'	108° 15'	0.40
30. Redfern and Herd Redfern and Herd No. 5	36° 40'	107° 59'	0.46

Table 1 (continued)

31. Sunray Mid-Continent Gallegos No. 122	36° 40'	108° 09'	0.49
32. El Paso Natural Gas S.J.U. 28-4 No. 28	36° 39'	107° 17'	0.67
33. Aztec Oil and Gas Reid No. 23-D	36° 39'	107° 49'	0.50
34. Aztec Oil and Gas Caine No. 13	36° 39'	107° 55'	0.44
35. Pan American Holder No. 7	36° 39'	108° 14'	0.46
36. El Paso Natural Gas S.J.U. 28-5 No. 50	36° 38'	107° 23'	0.55
37. El Paso Natural Gas Florence No. 10-C	36° 38'	107° 43'	0.43
38. Royal Development Ojo Amarillo No. 2	36° 36'	108° 16'	0.49
39. El Paso Natural Gas Rincon Unit No. 177	36° 35'	107° 32'	0.43
40. El Paso Natural Gas Schwerdtfeger No. 20-A	36° 35'	107° 42'	0.48
41. Aztec Oil and Gas Whitley No. 6-D	36° 35'	107° 49'	0.48
42. Aztec Oil and Gas Hanks No. 14-D	36° 35'	107° 52'	0.45
43. British-Amer. Oil Fullerton No. 8	36° 35'	107° 58'	0.45
44. El Paso Natural Gas S.J.U. 27-5 No. 74	36° 33'	107° 21'	0.50
45. El Paso Natural Gas Rincon Unit No. 171	36° 33'	107° 29'	0.49
46. Aztec Oil and Gas Hudson No. 5-D	36° 33'	107° 49'	0.44
47. Southwest Prod. Cambell No. 2	36° 33'	108° 05'	0.39

Table 1 (continued)

48. El Paso Natural Gas S.J.U. 27-4 No. 3	36° 32'	107° 17'	0.48
49. Caulkins Oil State "A" MD No. 62	36° 31'	107° 27'	0.44
50. Southwest Prod. Ted Henderson No. 1	36° 31'	108° 01'	0.37
51. Kay Kimbell Leiberman No. 5	36° 28'	107° 36'	0.44
52. Standard of Texas State No. 1	36° 24'	108° 13'	0.66
53. Merrion and Assoc. Federal No. 3-35	36° 22'	107° 27'	0.38
54. Century Exploration Mobil-Rudman No. 2	36° 22'	107° 48'	0.44
55. Dorfman Production Nancy Fed. No. 1	36° 18'	107° 39'	0.38
56. El Paso Natural Gas Lindrith No. 42	36° 17'	107° 08'	0.37
57. Val Reese and Assoc. Lybrook No. 7-27	36° 17'	107° 34'	0.40
58. Val Reese and Assoc. Bobby "B" No. 2-31	36° 16'	107° 30'	0.39
59. N.M.P.S.C.C. DH-32-1	36° 16'	108° 15'	0.54
60. N.M.P.S.C.C. DH-3-2	36° 14'	108° 12'	0.59
61. Val Reese and Assoc. Betty "B" No. 1-15	36° 13'	107° 35'	0.42
62. Fruitland outcrop	35° 54'	107° 02'	0.31
63. Fruitland outcrop	35° 54'	107° 14'	0.42
64. Fruitland outcrop	35° 53'	107° 05'	0.37
65. Pit sample	35° 53'	107° 22'	0.30

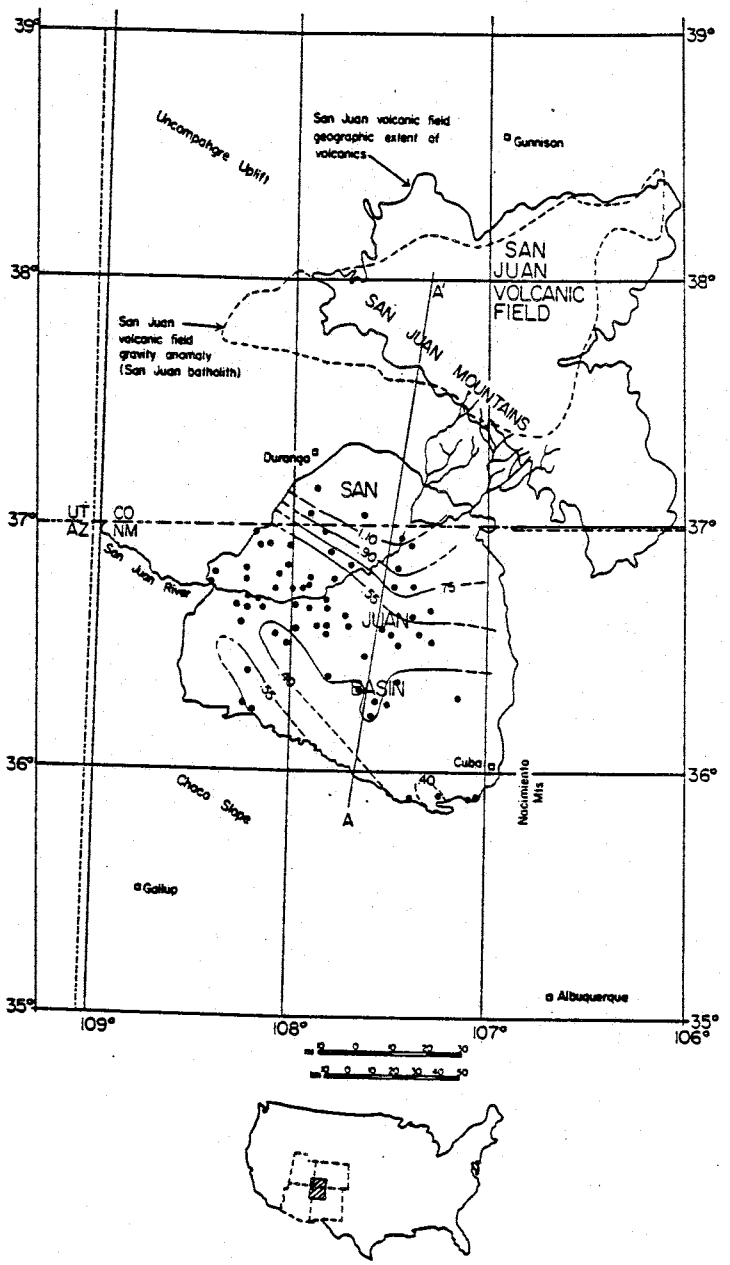

Figure 2. Location of coal maturation data sites and % vitrinite reflectance contours (after Fassett and Hinds, 1971).

vitrinite reflectance values using the scales in the International Handbook of Coal Petrography (1963), Dow (1978), and Heroux et al (1979). Two data points shown by Fassett and Hinds (1971) on the northern edge of the San Juan Basin were not used in this study as no information concerning the points was tabulated by these authors. The two maturation values not used are somewhat lower than other values in the northern Basin, probably due to shallow burial depths of the Fruitland coals along the northern edge of the Basin. Additional coal maturation data across the San Juan Basin were also shown by Rice (1983). The maturation values shown by Rice (1983) are in general agreement with the values of Fassett and Hinds (1971), however these values were also not used in this study as no information concerning the values was tabulated by Rice (1983). A trend of increasing R_o values can be noticed across the San Juan Basin as the San Juan Mountains are approached (Figure 2). This trend in the R_o values is indicative of the increased heating of Fruitland coals in the northern San Juan Basin (Reiter and Clarkson, 1983b; Rice, 1983).

Deep heat-flow data (temperature gradients measured to depths greater than 750 m) from the San Juan Basin were used in the present study (Table 2, Figure 3; Sass et al, 1971; Reiter et al, 1975; Reiter and Mansure, 1983). These values are thought to be more representative than shallow measurements in the Basin (Reiter and Mansure, 1983). Deep heat-flow data are unavailable in the San Juan Mountains

Table 2. San Juan region heat-flow data. Values used to calculate the average San Juan volcanic field heat flow are indicated by an *. Values used to calculate the average southern San Juan Basin heat flow are indicated by a +.

Well	North Latitude	West Longitude	Heat Flow (mW/m^2)	Reference
1. Nellie Creek	38° 04'	107° 23'	128*	Reiter et al, 1975
2. Mary Alice Creek	38° 03'	107° 30'	144*	Reiter et al, 1975
3. Ouray	37° 56'	107° 40'	150*	Decker and Birch, 1974
4. Silverton	37° 48'	107° 37'	93*	Reiter et al, 1975
5. Del Norte	37° 47'	106° 22'	113*	Decker and Bucher, 1979
6. Rico 1	37° 42'	108° 01'	218-247*	Decker and Bucher, 1979
7. Rico 2	37° 42'	108° 02'	218-255*	Decker and Bucher, 1979
8. Chicago Basin	37° 36'	107° 37'	103*	Decker and Bucher, 1979
9. V Basin 1	37° 34'	107° 35'	96*	Decker and Bucher, 1979
10. V Basin 2	37° 34'	107° 35'	88*	Decker and Bucher, 1979
11. Summitville	37° 26'	106° 36'	100*	Decker and Bucher, 1979
12. Summitville DDH-SM31	37° 26'	106° 36'	103*	Decker and Birch, 1974
13. Alum Creek	37° 25'	106° 30'	92*	Edwards et al, 1978

Table 2 (continued)

14.	Pagosa Springs: G-1	37° 15'	107° 01'	199*	Galloway, 1980
	G-2			174*	
	G-3			150*	
	G-4			124*	
	G-5			128*	
	G-6			90*	
15.	Bondad	37° 09'	107° 55'	115	Reiter and Mansure, 1983
16.	Southern Ute	37° 03'	107° 48'	99	Reiter and Mansure, 1983
17.	Allison 59	37° 00'	107° 31'	96	Reiter and Mansure, 1983
18.	Kelly	36° 54'	107° 51'	90	Reiter and Mansure, 1983
19.	Com G8	36° 51'	107° 41'	91	Reiter and Mansure, 1983
20.	Carson Forest	36° 49'	107° 14'	92	Reiter and Mansure, 1983
21.	Atlantic State	36° 48'	107° 53'	87	Reiter and Mansure, 1983
22.	Fed. No. 1	36° 44'	108° 17'	70	Reiter and Mansure, 1983
23.	Roelofs A1A	36° 42'	107° 39'	82	Reiter and Mansure, 1983
24.	Gobenador	36° 41'	107° 12'	84	Sass et al, 1971
25.	San Juan Unit 28-6-20R	36° 38'	107° 25'	83	Reiter and Mansure, 1983
26.	San Juan Unit 27-4-73	36° 34'	107° 16'	83	Reiter and Mansure, 1983
27.	Jicarilla F1A	36° 33'	107° 07'	89	Reiter and Mansure, 1983
28.	Angel Peak	36° 33'	108° 02'	73	Reiter and Mansure, 1983

Table 2 (continued)

29. Bisti	36° 25'	108° 02'	69	Reiter and Mansure, 1983
30. Canyon Largo	36° 24'	107° 25'	69	Reiter and Mansure, 1983
31. Gavilon	36° 22'	106° 54'	72	Reiter and Mansure, 1983
32. Sixteen G	36° 19'	107° 49'	70	Reiter and Mansure, 1983
33. Chaco Canyon	35° 57'	107° 54'	64+	Reiter and Mansure, 1983
34. Star Lake	35° 56'	107° 28'	70+	Reiter and Mansure, 1983
35. Media Entrada	35° 52'	107° 10'	72+	Reiter and Mansure, 1983
36. Chaco Slope	35° 51'	107° 24'	62+	Reiter et al, 1975
37. Crownpoint	35° 51'	108° 03'	67+	Reiter and Mansure, 1983

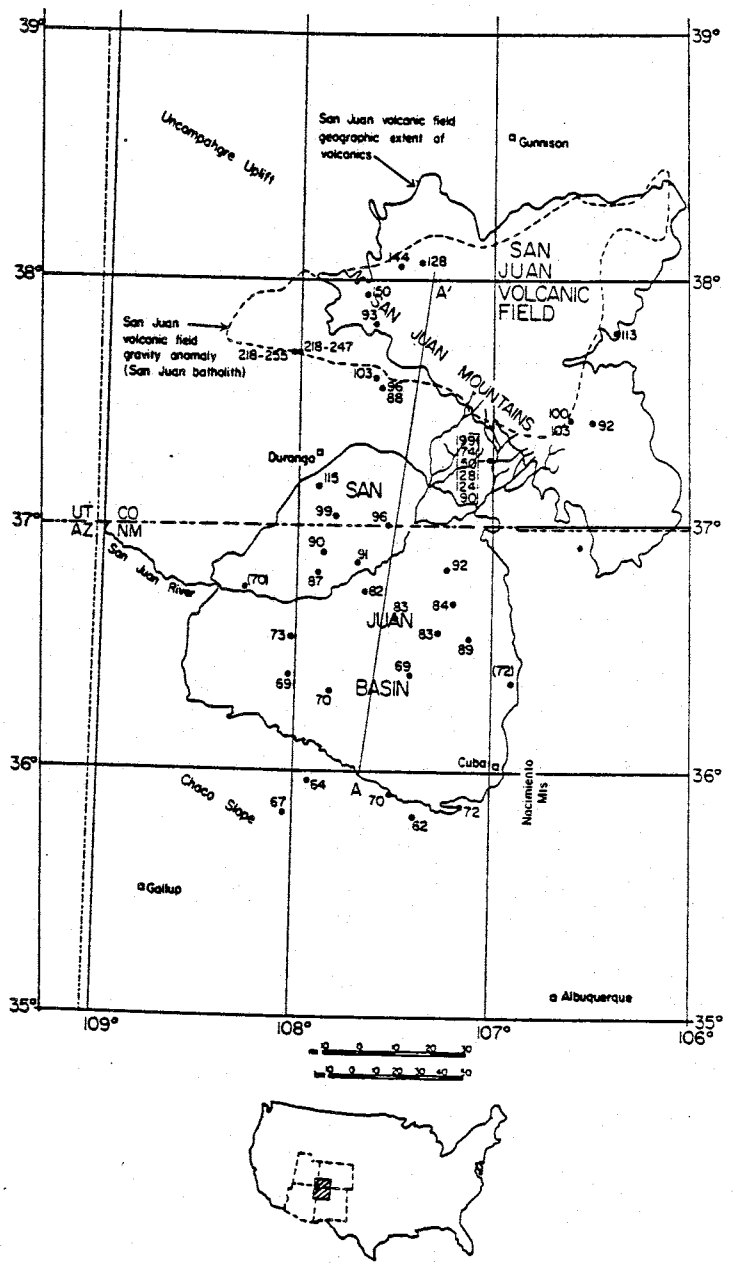

Figure 3. Heat-flow values and location of data sites. Deep-data sites (temperature gradients measured to >750 m) are indicated in the San Juan Basin. All available data sites are shown in the San Juan volcanic field.

region, therefore all available heat-flow data were used to obtain an average value (Table 2, Figure 3). For purposes of obtaining an average regional value, heat-flow data from sites within one minute of latitude and longitude of one another were averaged to give a single heat-flow value for that location. The mean of the values from all locations in the San Juan Mountains region (127 mWm^{-2}) was then taken to represent the regional heat flow. The regional heat flow in the southern San Juan Basin was taken to be the average of the five heat-flow values located just outside the southern Basin (67 mWm^{-2}; Table 2, Figure 3).

The observed heat-flow data were projected onto a profile line (Figure 3, AA') so that comparisons could be made to heat-flow values predicted from thermal models. The profile line was determined by least squares fitting the data sites used in the study, minimizing longitude variations. (The heat flow values shown in parentheses in Figure 3 were not projected onto the profile line as they were outside two standard deviations of the least squares line.) Data sites are projected onto the profile line in two different manners: along lines of latitude and along coal maturation contours (Figures 4a and 4b). Note that the trend of observed heat flow resulting from the latter projection is perhaps a smoother trend; this implies a compatability between present heat flow and the level of coal maturation. The major conclusions of the study will be the same for either of the projections shown in Figure 4.

Note the increasing heat flow from south to north across the San Juan Basin as the San Juan Mountains are approached.

Basic Principles of the Thermal Models

Heat flow

In order to study the thermal regime of the San Juan region time-dependent heat-flow models were constructed using finite difference techniques. Details of the modelling are presented in Appendix 1. The time-dependent models used were two dimensional with isothermal upper and lower boundaries and no-flux side boundaries (Figure 5). Thermal conductivity and radiogenic heat production as a function of depth are important model parameters. These model parameters are also presented in Figure 5. Thermal conductivity and heat production were assumed to be laterally homogeneous. The assumption of lateral homogeneity simplifies the modelling and appears reasonable based on the data available for the San Juan region (Reiter and Mansure, 1983). A further discussion of the model parameters is presented in Appendix 1. Model temperatures were determined by assigning a temperature and step height to the lower isotherm and calculating the resulting temperature distribution with time (Appendix 1).

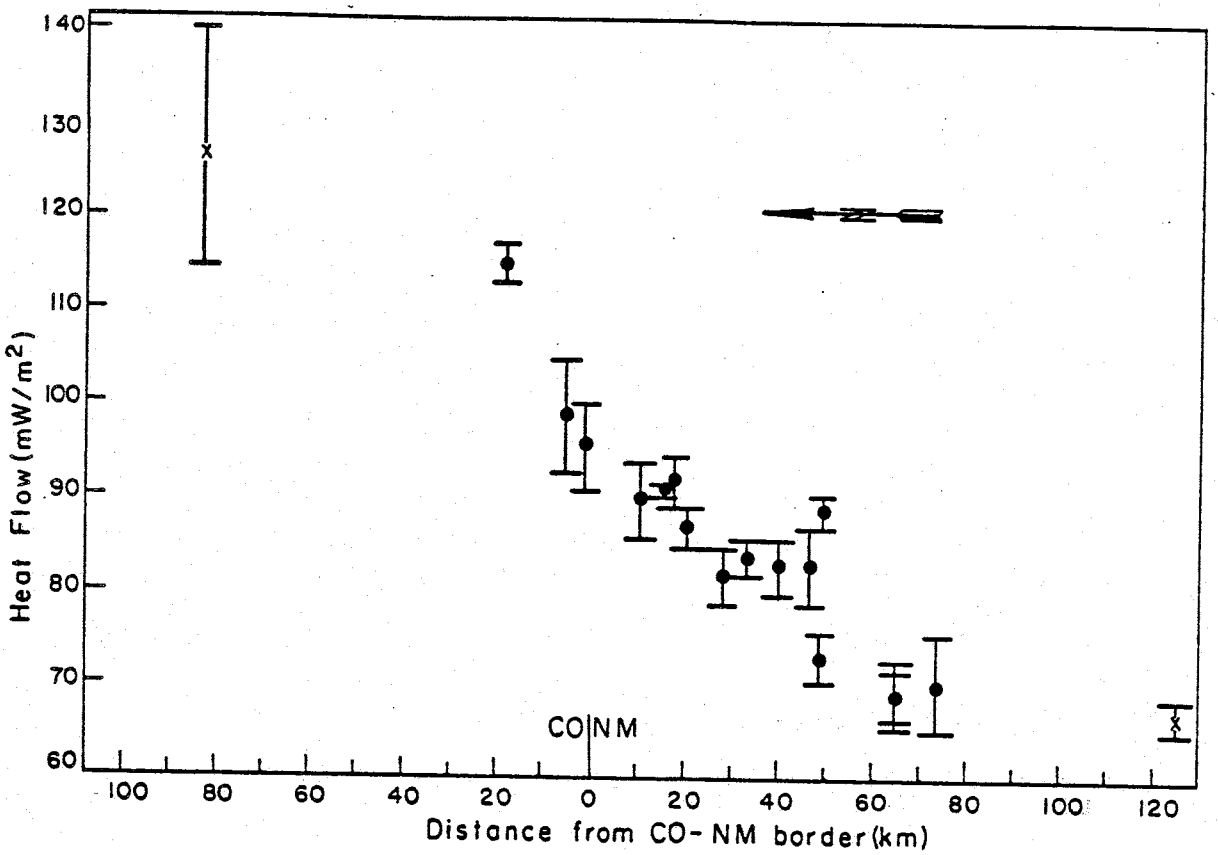

Figure 4a. San Juan Basin heat-flow values projected onto profile line AA' (Figure 3) following the latitude of the data sites. The x's indicate the average heat flow in the San Juan Mountains and southern San Juan Basin. Error bars indicate the standard error associated with the heat flow values.

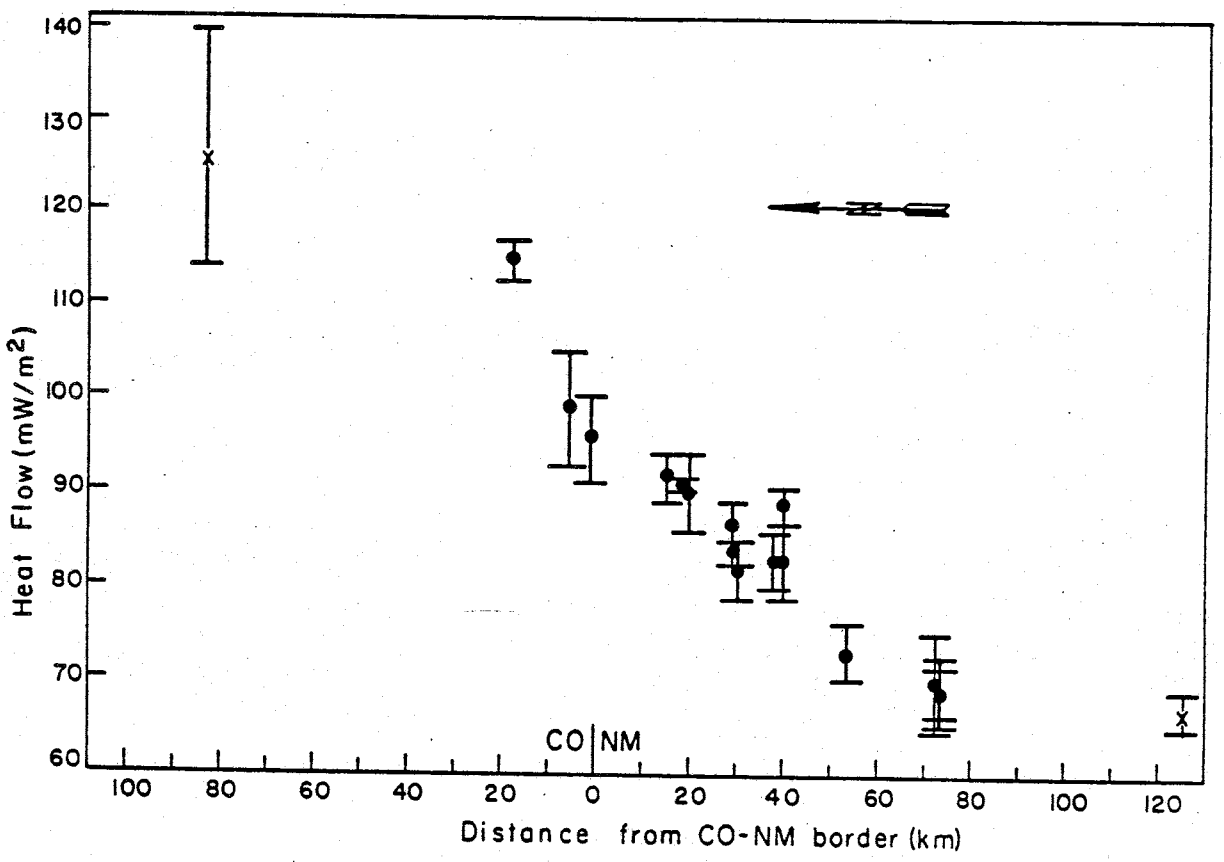

Figure 4b. San Juan Basin heat-flow values projected onto profile line AA' (Figure 3) following the coal maturation contours. The x's indicate the average heat flow in the San Juan Mountains and southern San Juan Basin. Error bars indicate the standard error associated with the heat flow values.

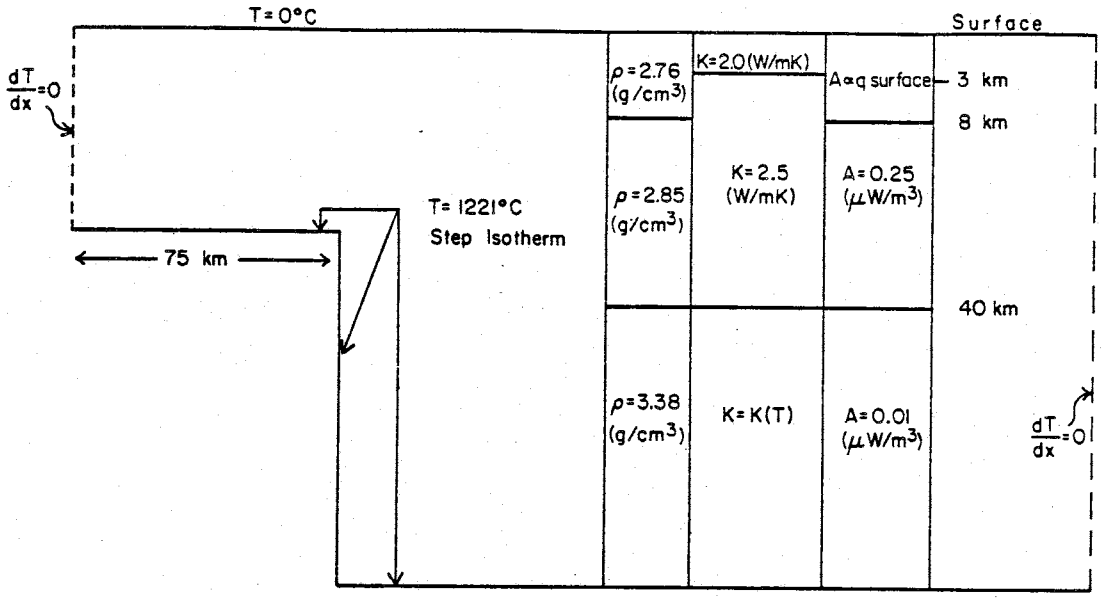

Figure 5. Illustration of step model and parameters employed in temperature calculations. Conductivity below 40 km is temperature dependent, following the model of Schatz and Simmons (1972). Radiogenic heat production from 0-8 km is assumed to provide 40% of the observed surface heat flow (Chapman and Pollack, 1977). See Appendix 1 for a detailed discussion of the model.

As mentioned above, the observed heat flow in the San Juan region provides a constraint for the time dependent temperature models, i.e. the models must predict a present heat flow consistent with the observed heat flow. Observed heat-flow values at the endpoints of the profile across the Basin (127 mWm^{-2} for the San Juan Mountains area and 67 mWm^{-2} for the southern San Juan Basin) are taken to represent average regional heat flows for the respective areas. Therefore any acceptable thermal model should be consistent with these endpoint heat-flow values. Acceptable models can then be defined by the fit between predicted heat flows and observed heat flows in the transitional region between the endpoints.

The thermal models studied had a step discontinuity in the lower isotherm (Figure 5). The temperature of the lower isotherm was taken to be about 1200 ^{o}C, the approximate upper limit to magma temperatures (Jaeger, 1964). Steady-state temperature distributions resulting from a step discontinuity were initially studied. Depths to the shallow and the deep parts of the step were chosen so that the endpoint values of ~127 mWm^{-2} and ~67 mWm^{-2} were obtained. The lateral position of the step discontinuity was then varied relative to the observed heat-flow sites in order to find a best least mean squares fit between the predicted and observed heat-flow values. Figure 6 presents the best-fit steady-state temperature model.

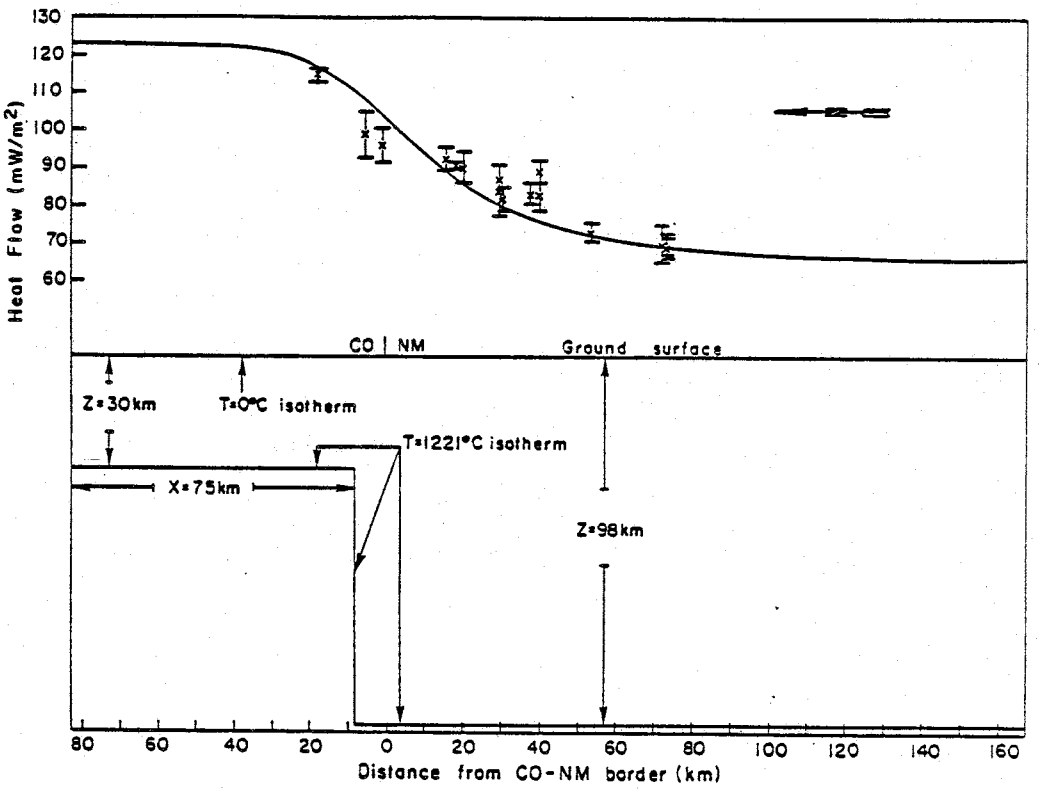

Figure 6. Best-fit steady-state isothermal step model and resulting calculated heat-flow profile. The calculated profile is compared with the observed heat-flow values. The heat-flow data sites are projected onto line AA' (Figure 3) using the coal maturation contours (Figure 4b). Error bars indicate standard error associated with the heat flow values.

In order for the steady-state model to be reasonable, sufficient time must elapse since the initiation of a thermal event (emplacement of the isothermal step). For the best-fitting steady-state model, Figure 7 presents the change of model heat-flow curves with time, assuming that the isothermal step is instantaneously emplaced into a region having a heat flow of 67 mWm^{-2} (the mean heat flow in the southern San Juan Basin). The steady-state temperature distribution is closely approached after 20 my. Times on the order of 30-40 my since the initiation of a thermal event in the San Juan region would be reasonable in view of the extensive Oligocene volcanism which began about 35 mya and the Laramide volcanism which began about 70 mya. Other temperature histories which approach the steady-state distribution would also be reasonable, however the observed heat flow (representing present thermal conditions) will not distinguish between such models. As will be discussed later, different models can be evaluated using the geologic history and level of coal maturation in the region.

Transient temperature distributions were also examined to see if a better fit to the observed San Juan region heat flow could be obtained, i.e. a fit better than the steady-state model fit. From Figure 6 it may be seen that a model heat-flow curve broader than the best-fit steady-state curve would better fit the observed heat flow in the San Juan region. Broader heat-flow profiles may be generated by models having deeper isothermal steps (i.e. deeper than the

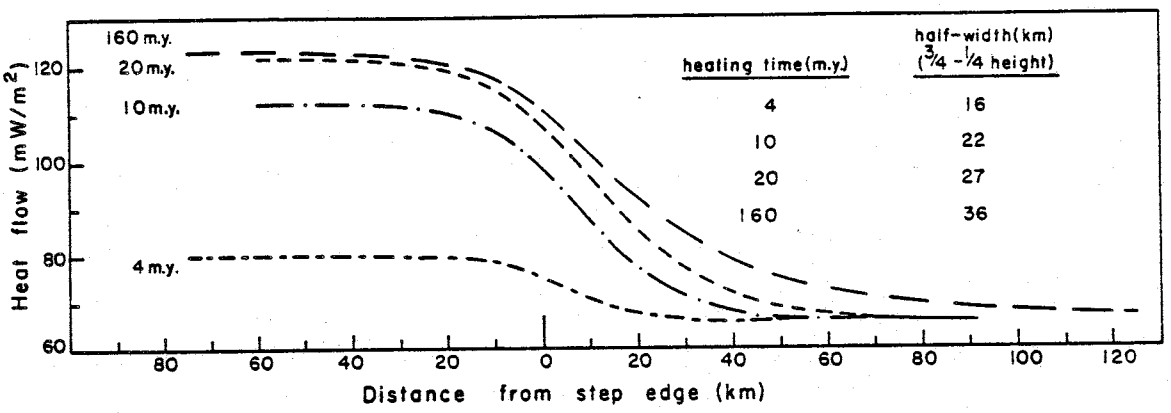

Figure 7. Change of surface heat-flow profile with time for a lower isothermal step extending from 30 to 98 km depth (as in the best fit model) emplaced into a region with an initial uniform heat flow of 67 mWm^{-2}.

best-fit steady-state model), however the endpoint heat flows will be inconsistent with the observed values unless the endpoint values occur during transient times. Various transient thermal models are discussed below.

Heat-flow curves for two cooling models in which the initial temperature distribution results from a steady-state isothermal step 10 to 98 km deep are shown in Figures 8a and 8b. Figure 8a presents the variation of heat flow when the upper part of the step is lowered instantaneously from 10 to 40 km depth; Figure 8b shows the heat-flow variation when the step is lowered instantaneously from 10 to 98 km. For these models the heat-flow profile broadens as cooling occurs, the final curve width being determined by the final steady-state conditions. For the case shown in Figure 8a the heat-flow profile broadens from a half width of 14 km to 44 km and for the case shown in Figure 8b the initial profile with a 14 km half width becomes a flat profile (with a constant value of 67 mWm^{-2}) in the steady state. For cooling models in which the shallow part of the final step isotherm is deeper than 30 km the heat-flow profile will at some time be broader than the best-fit steady-state model heat-flow curve presented in Figure 6; however, this broader curve occurs long after the model projects the necessary endpoint heat flow of 127 mWm^{-2}.

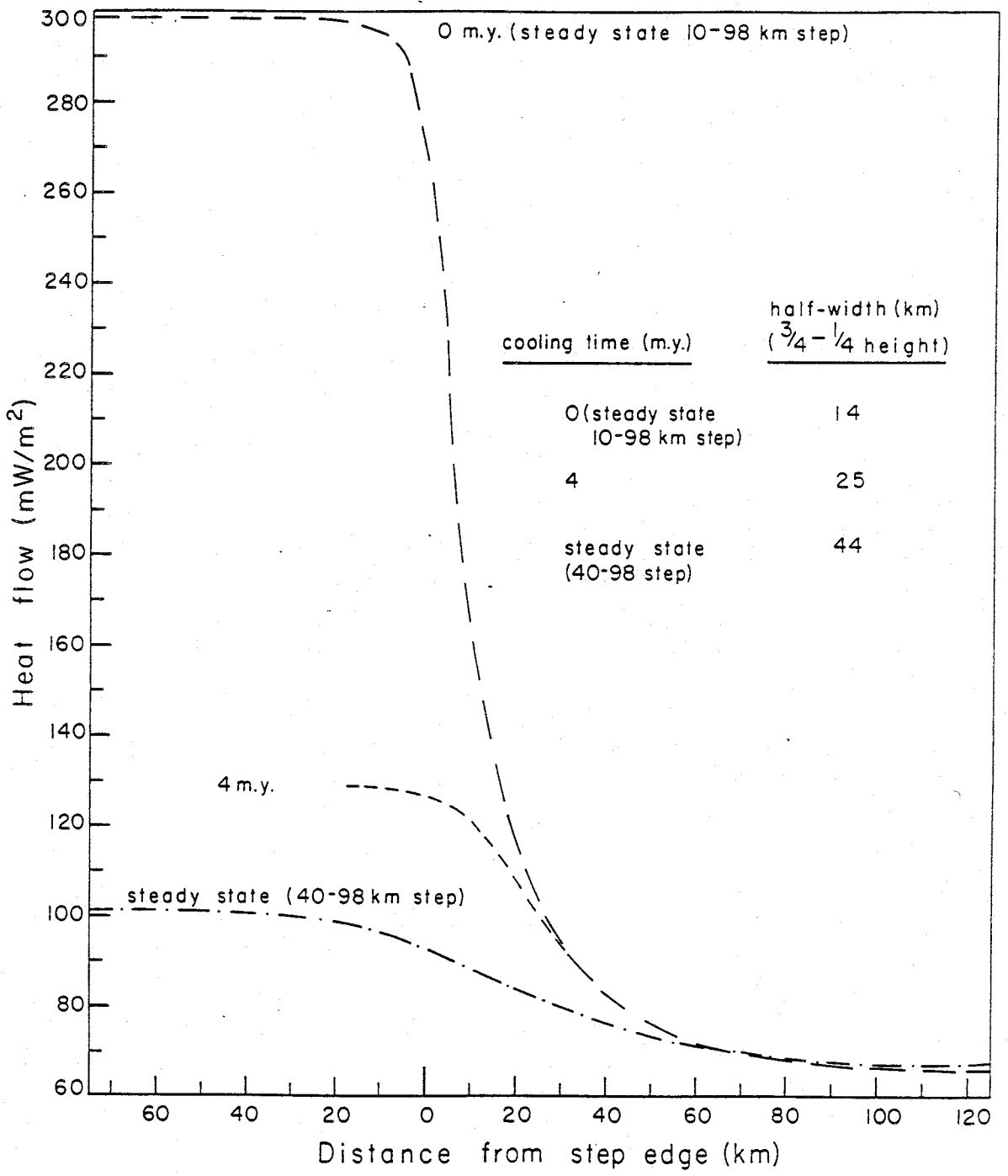

Figure 8a. Change of surface heat-flow profile with time for a cooling model. Initial temperature distribution results from an isothermal step extending from 10 to 98 km depth. At t=0 the initial step isotherm is instantaneously lowered to an isothermal step extending from 40 to 98 km depth.

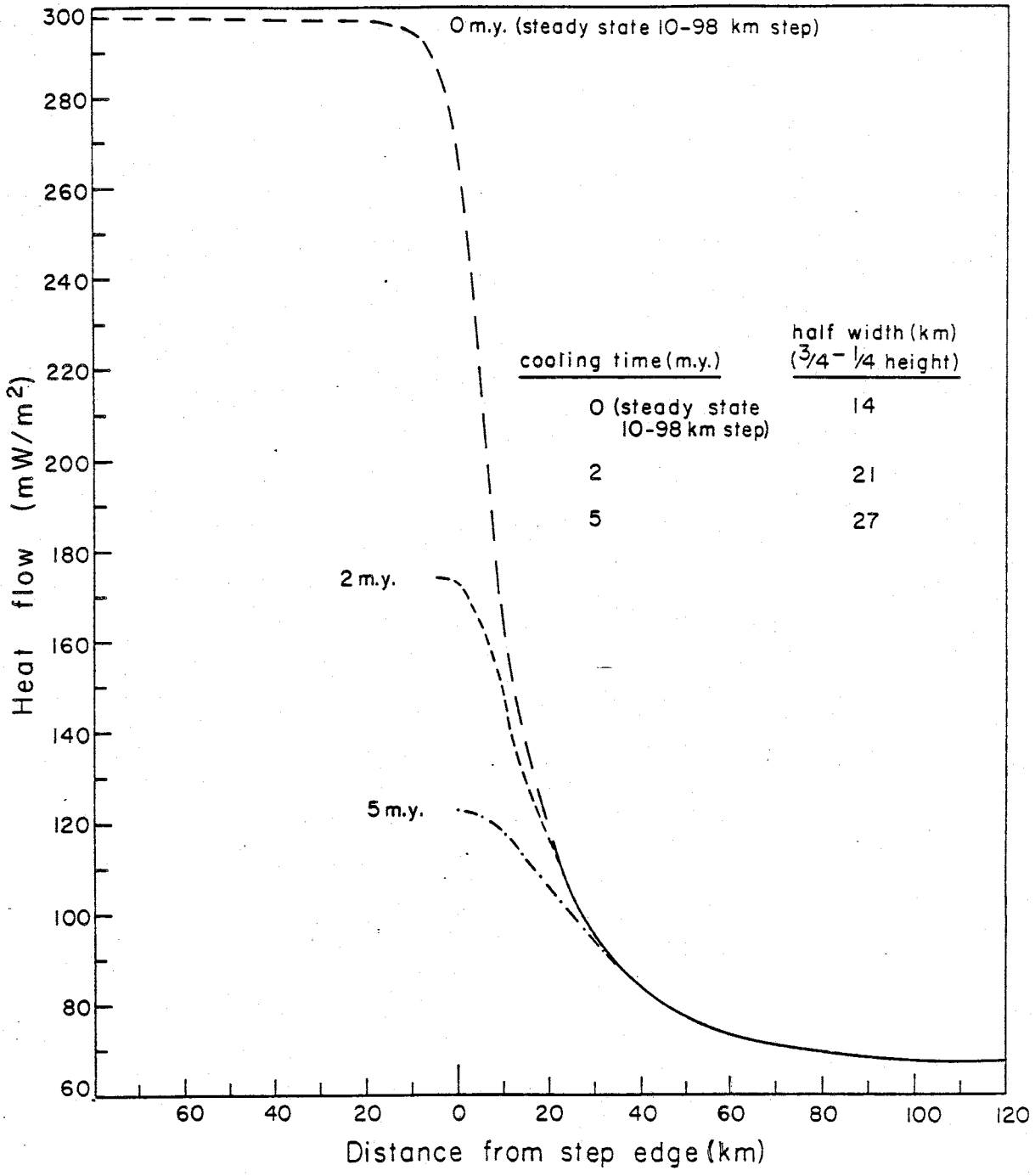

Figure 8b. Change of surface heat-flow profile with time for a cooling model. Initial temperature distribution results from an isothermal step extending from 10 to 98 km depth. At t=0 the initial step isotherm is instantaneously lowered to a flat isotherm at 98 km depth.

Figure 9 presents heat-flow curves for a warming model in which an isothermal step, 20 to 98 km depth, is instantaneously emplaced into a region with a heat flow of 67 mWm^{-2}. The heat-flow curve broadens with time, reaching a steady-state half-width of 26 km. This model will not fit the observed San Juan heat flow better than the best-fit steady-state model. Note when the endpoint heat-flow value of 127 mWm^{-2} is obtained (3 my after the emplacement of the isothermal step at 20 km depth) the heat-flow curve has only a 13 km half-width, as compared to the 36 km half-width for the best-fit steady-state model.

Figures 10a and 10b present heat-flow curves for two other warming models having an initial isothermal step deeper than the best-fit steady-state model. The upper part of the isothermal step is instantaneously raised to a depth shallower than 30 km. Again the endpoint heat-flow value (127 mWm^{-2}) and the width of the heat-flow curve are such that the fit of the model curves to the observed heat flow is not as good as with the steady-state model; i.e., the endpoint heat-flow values and the heat-flow profile half widths are incompatible with the observed values.

From the above discussion it may be concluded that the best fit between any isothermal step model and the observed San Juan region heat flow is obtained with the steady-state model. Any temperature history which approaches the above steady-state model in the present would also be a reasonable

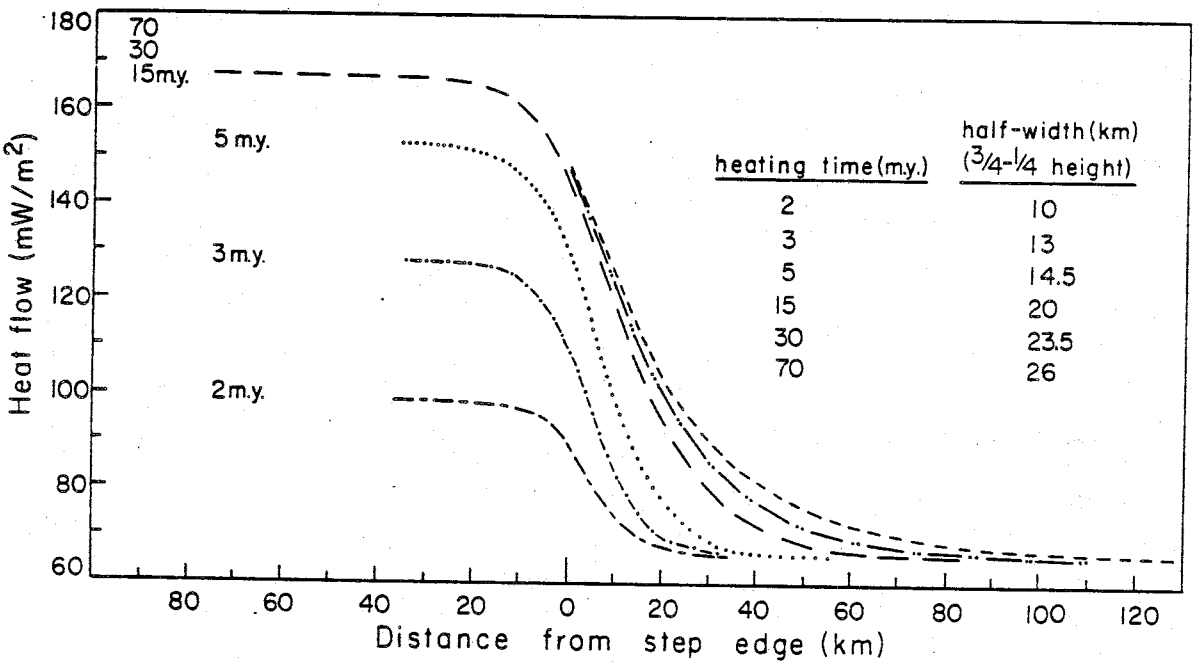

Figure 9. Change of surface heat-flow profile with time for a lower isothermal step extending from 20 to 98 km depth emplaced into a region with an initial uniform heat flow of 67 mWm^{-2}.

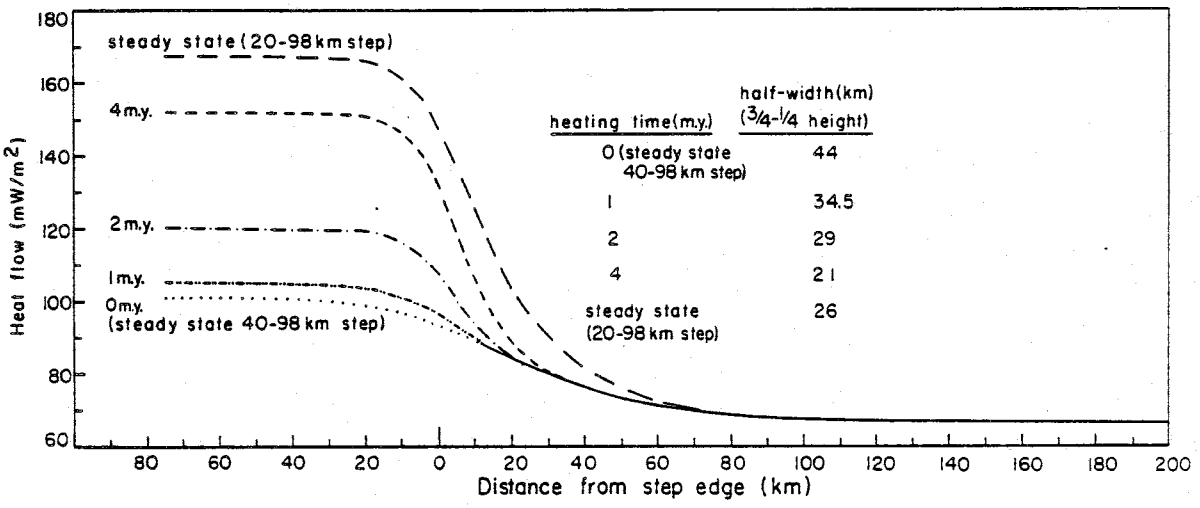

Figure 10a. Change of surface heat-flow profile with time for a warming model. Initial temperature distribution results from an isothermal step extending from 40 to 98 km depth. At t=0 the initial step isotherm is instantaneously raised to an isothermal step extending from 20 to 98 km depth.

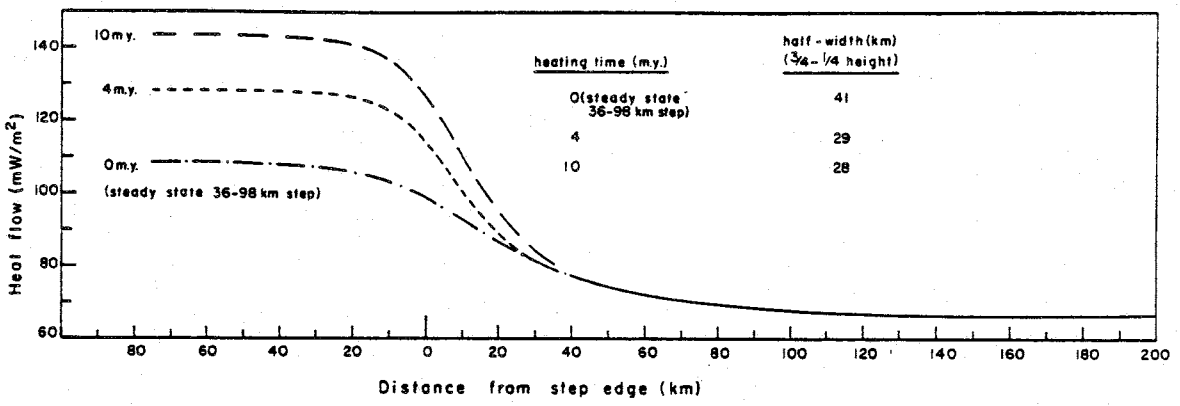

Figure 10b. Change of surface heat-flow profile with time for a warming model. Initial temperature distribution results from an isothermal step extending from 36 to 98 km depth. At t=0 the initial step isotherm is instantaneously raised to an isothermal step extending from 24 to 98 km depth.

model. More complicated model geometries may be introduced to attempt a better fit of predicted heat-flow profiles to observed data. For example a model in which the vertical part of the isothermal step had a slope would broaden the resulting heat-flow profiles. Three-dimensional models could also be considered, however Reiter and Clarkson (1983a) show that the differences in the location of the elevated temperature region, the depths to the lower isotherm, and the fit to the observed heat-flow data for cylindrical (three dimensional) and step (two dimensional) models are minor for steady-state models. More complicated models may not be justified with the present data resolution, e.g. the measured heat-flow profile may be influenced by regional ground-water movement. The above steady-state model gives a reasonable fit to the observed heat flow.

Even if the San Juan region is not in steady state, the present near surface temperature regime would be approximated by the steady-state temperature distribution, although deeper temperatures may be subject to greater uncertainties. The near surface temperatures will be fundamental in calculating the level of coal maturation in the San Juan Basin.

Although the primary purpose of this study is to model the effects of the thermal history on the coal maturation across the San Juan Basin, it may be of some interest to

speculate on possible sources of the modelled steady-state temperature distribution. As noted above, the depth to the isothermal step for the steady-state model requires ~20 my of heating to approximate the steady-state condition. The steady-state isotherm could result from a single source which has been active for at least 20 my. The isotherm could also result from more than one source whose cumulative effects approximate the steady-state case. For example, although the thermal effects of the Laramide and Oligocene activity in the San Juan Mountains may not produce the present thermal conditions in the region, the activity may have "pre-heated" the crust in the region, allowing the steady-state condition to be more readily approximated in Miocene and later times.

The geometry, temperatures, and time scale of the steady-state model suggest that the basic thermal source involved is the advection of heat from the mantle into the crust. The convective rise of mantle material in plumes as described by Morgan (1972) to explain the presence of "hot spots" on the earth's surface is one type of advecting mechanism. The San Juan Mountains are similar in some respects to the Yellowstone region of the United States, an area of high heat flow and recent magmatic activity, which has been suggested as a possible hot-spot location (Morgan, 1972; Iyer, 1979). Teleseismic delays and gravity data in the Yellowstone region have been used to suggest a large magma body underneath the Yellowstone caldera which is in

turn underlain by a region of partial melting that extends to at least 100 km depth, and possibly to 250 km depth (Eaton et al, 1975; Iyer, 1979). The San Juan Mountains are similar to the Yellowstone region in that they have a large negative Bouger gravity anomaly (Plouff and Pakiser, 1972; Eaton et al, 1975), perhaps associated with near surface magma and volcanic rock; and a small positive free air gravity anomaly (Kaula, 1970), perhaps associated with the rise of mantle material beneath the areas. From a refraction survey which crossed near the eastern end of the San Juan Mountains, Prodehl and Pakiser (1980) suggest a velocity inversion in the upper crust which may be due to elevated temperatures at depth. Although there are similarties between the Yellowstone and San Juan Mountains regions, it is difficult to explain the thermal history of the San Juan Mountains since at least Oligocene time by just a hot-spot mechanism because the motion of the North American plate since Oligocene time would cause the San Juan region to be removed from the source of heat.

Mantle diapirism in association with subduction is another mechanism for advecting heat from the mantle to the crust. Diapirism may occur as a result of frictional heating along the subducting slab or as the result of flow induced in the mantle by the subducting slab (Turcotte and Schubert, 1982). With this mechanism the location of the heat source will be a function of the relative position of the subducted lithosphere and the overlying plate, thus

eliminating the problem of the plate motion removing the San Juan region from the heat source. Subduction related magmatism was suggested by Lipman et al (1978) as the cause of the Oligocene volcanism in the San Juan Mountains. It was noted above however that the heat flow in the San Juan region requires a source which is larger than the San Juan batholith. It could be that the subduction related magmas rose to the base of the lithosphere in the San Juan region and have thinned the lithosphere, or been injected into it, producing the observed thermal anomaly. The lack of extensive volcanism except in conjunction with the emplacement of the San Juan batholith may be related to local stress conditions and/or to an inherent lithospheric weakness in the San Juan Mountains. The recurrent tectonic and magmatic activity in the region since at least late Paleozoic time (Tweto, 1975) may be an indication of lithospheric weakness in the region. However, relative plate motions may make it difficult to relate the more recent magmatic activity in the San Juan region to subduction along western North America.

Thinning of the lithosphere, allowing the mantle to rise is another mechanism which could produce the observed heat flow in the San Juan region. Lithospheric thinning could be related to tensional stresses in the region, which have existed since Miocene time (Lipman et al, 1978). Tensional stresses can cause instability in the mantle and thus induce diapiric upwelling (Turcotte and Emerman, 1983).

Thinning of the crust and upwarping of the mantle has been postulated in tensional rift environments, such as the Rio Grande rift (Bridwell, 1976; Cordell, 1978; Keller et al, 1979; Lipman and Mehnert, 1979; Olsen et al, 1979). The heat flow profile from south to north across the San Juan region is rather similar to the heat flow profile from the Rio Grande rift west to the San Juan Basin, perhaps suggesting a similarity in the heat sources for the two regions (Clarkson and Reiter, 1984). Estimates based on the models of Lachenbruch and Sass (1978) suggest that extension rates of 1-3%/my could produce the observed San Juan Mountains heat flow (127 mWm^{-2}); although such extension over the past 20 my is questionable, especially in the northern San Juan Basin.

It may be that the present thermal conditions in the San Juan region result from a combination of the latter two mechanisms; that is, heating associated with the rise of magmas related to subduction in Oligocene time followed by diapiric rise of the mantle in association with tensional stresses and lithospheric thinning. This combination of events would agree with the origin of magmas in the San Juan Mountains proposed by Lipman et al (1978). The more recent heating could be causally or only temporally related to the Oligocene activity. For example, the Oligocene magmatism may have generated a tensional environment as the lithosphere thinned, initiating upwelling in the mantle after the subducting plate ceased to be a heat source in the

region. Alternatively, the tensional stresses in the region may result from causes unrelated to the Oligocene magmatism, although previous heating of the lithosphere during Oligocene time would aid mantle flow during later times (Mareschal, 1983).

Coal maturation

The time-temperature index of hydrocarbon maturation (after Waples, 1980) was employed to model maturation levels of the Fruitland Formation coals in the San Juan Basin. Using this method various thermal histories for the San Juan region may be evaluated by comparing the coal maturation values calculated for a given thermal history to the observed coal maturations in the San Juan Basin. The method represents the level of hydrocarbon maturation as

$$TTI = \sum_{n} 2^{n} \Delta t$$

where t is the time of exposure to a temperature within the nth 10 ^{o}C temperature interval. Waples (1980) arbitrarily chose n=0 for T=100-110 ^{o}C and correlated the TTI values to vitrinite reflectance. This method was modified slightly in the present study by considering maturation to be a continuously varying function of temperature and time, i.e.

$$TTI = \int 2^{[T(t)-105]/10} dt.$$

(See Appendix 2 for further discussion of thermal maturation.)

Because the maturation of coal is temperature dependent it becomes necessary to estimate parameters affecting the temperature within the earth, e.g. the geothermal gradient, the depth of burial and the surface temperature. Coal maturation is also time dependent, it therefore becomes necessary to estimate the above parameters through time. To investigate the thermal history of the San Juan Basin the present study uses the maturation values of the coals of the Fruitland Formation which were deposited about 75-71 mya (Molenaar, 1983; Fassett and Hinds, 1971). Thus it will be necessary to estimate the above parameters for the past 73 my in order to calculate a level of coal maturation for any given thermal model.

Surface temperature effects can be important in determining maturation temperatures for coals with shallow burial depths (0-2 km). Changes in surface temperature can result from both climatic and elevation changes. Sea level temperatures for the San Juan Basin over the past 73 my were estimated by projecting a sea level temperature for the San Juan Basin using Wolfe's (1978) paleotemperature curves for 4 other regions. Figure 11 shows the estimated sea level temperature for the San Juan Basin over the past 73 my.

The average elevation of the Coloardo Plateau as a whole is about 2 km (Bird, 1979). In the San Juan Basin region of the Colorado Plateau, the elevation ranges from 1.6 to 2.4 km (Fassett and Hinds, 1971). It has been

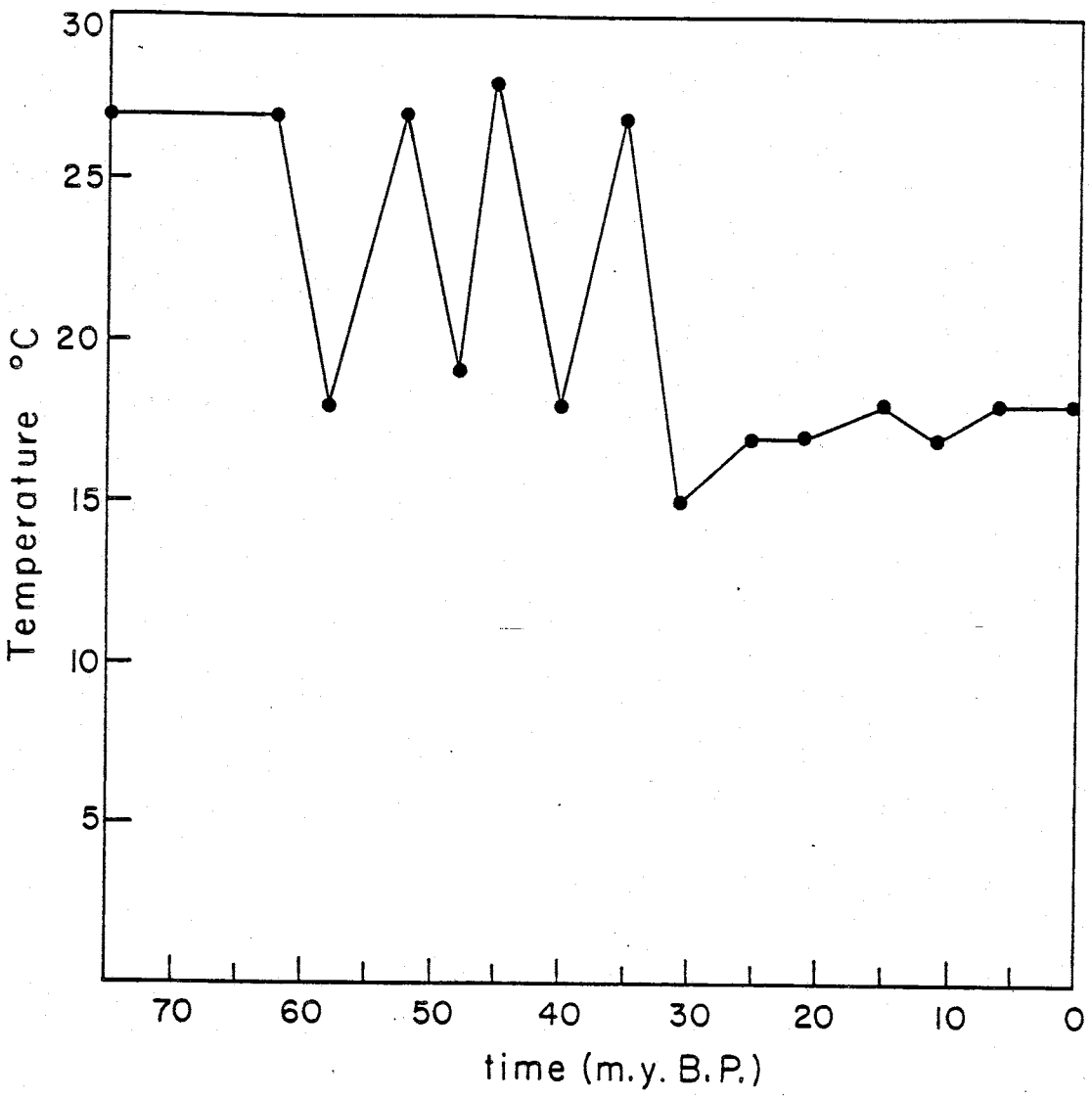

Figure 11. Estimate of the average paleotemperature at sea level in the San Juan Basin.

estimated that the Colorado Plateau had an average elevation of 1.2 km at the close of Laramide time (P.E. Damon, in Bird, 1979). The Grand Canyon region of the Plateau has been uplifted 0.9 km in the last 5.5 my (Lucchitta, 1979). The nearby southern Rocky Mountains were strongly uplifted between 7 and 4 mya (Chapin, 1979). It has also been estimated that the Colorado Plateau has been uplifted almost 2 km since Miocene time (C.E. Dutton, in Bodell and Chapman, 1982). Figure 12 presents the elevation models used in the calculation of coal maturation values. For a given geologic model the sea level temperature in the San Juan Basin was adjusted for elevation using a -6 ^{o}C/km atmospheric temperature gradient (Wright, 1966).

In order to evaluate possible thermal histories for the San Juan Basin, various maturation levels were calculated for the Fruitland Formation coals. These calculations result from different temperature models combined with various geologic models (elevation and burial depth models, Figure 12) which incorporate the estimated sea level surface temperatures for the San Juan Basin. Table 3 presents observed Fruitland Formation coal maturation values and maturation values calculated for various thermal and geologic models. The different temperature histories and the resulting calculated maturation values are discussed below. In the following discussion the northern San Juan Basin is defined as being north of the step edge (as defined by the best-fit steady-state isothermal step), the central

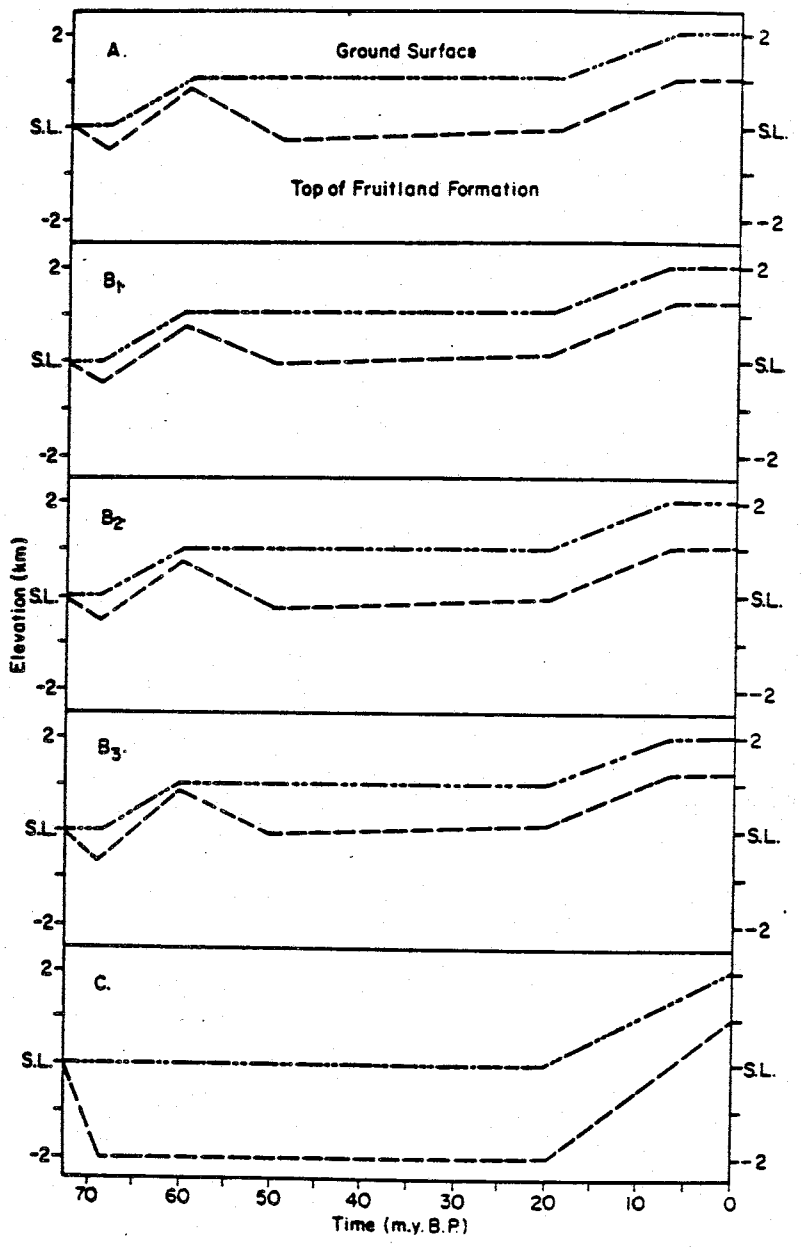

Figure 12. Ground surface and top of Fruitland Formation elevations used in the calculation of the model vitrinite reflectance values (Table 3). A and C are general San Juan Basin models. Model B_1 is for a location over the step edge (best-fit steady-state step) along the profile line (AA'), B_2 is for a location 25 km south of the step edge, and B_3 is for a location 75 km south of the step edge.

Table 3. Observed and calculated vitrinite reflectance values along the profile line (AA', Figure 3).

Distance from step edge[1] (km)	Observed Maturation (R_o)	Model[2,3] Maturation (R_o) I/A	II/A	II/C	I/B
-25	ND[4]	0.65	>2.20	ND	1.92
0	1.1-1.2	0.59	>2.20	1.39	1.62
25	1.0	0.51	0.52	0.51	1.04
50	0.55	0.47	0.45	ND	0.80
75	0.45	0.45	0.44	0.41	0.72
225	ND	0.42	0.43	ND	0.67

[1]Step defined by best-fit steady-state isothermal step model (see Figure 6). Distances north of step edge are considered to be negative.

[2]Temperature distributions used for calculation of maturation values:

I. temperatures from best-fit steady-state isothermal step model
II. temperatures from two-stage heating model.

[3]For the geologic models A, B, and C associated with the calculated maturation values see Figure 12.

[4]ND indicates that the maturation value was not determined at this location.

Basin is defined as being between 0 and 50 km south of the step edge, and the southern Basin is defined as being >50 km south of the step edge.

Model I/A (Table 3) presents calculated coal maturation values assuming the temperature distribution as defined by the best-fit steady-state model above, (Figure 6) in the San Juan region over the past 73 my and assuming a generalized San Juan Basin geologic history (Figure 12A). The calculated maturation value agrees with the observed maturation value in the southern San Juan Basin, an area of low maturation (Table 3). In the northern and central San Juan Basin, however the calculated coal maturation values are considerably less than the observed maturation values.

Greater coal maturation values for the central and northern San Juan Basin could be calculated if additional heating is proposed in association with the magmatic activity in the San Juan Mountains. Model II/A (Table 3, Figure 12A) presents calculated coal maturation values for a temperature model containing two major shallow heating episodes combined with the generalized Basin geologic history. This two stage heating model is similar to the best-fit steady-state isothermal step model except that the shallow part of the lower boundary isotherm was elevated to 10 km depth for the time periods 70-60 mya and 40-20 mya. The timing of the heating events was chosen to correspond approximately to the periods of magmatic activity in the San

Juan region. With this model the coal maturation values calculated for the northern San Juan Basin are greater than the observed values, the calculated values in the central Basin are less than the observed values, and the southern Basin coal maturation values again agree with the observed values.

The calculated maturation values for the San Juan Basin can be refined by considering a more local burial history. For example, Model II/C (Table 3, Figure $12B_1$, $12B_2$, and $12B_3$) uses three different burial histories for three locations in the Basin along profile line AA' (Figure 2). These histories were determined using stratigraphic information from nearby wells (see Figure 3 and Table 1) and more local burial histories (based on Fassett and Hinds, 1971). Maturation values calculated for the three locations using the more local burial histories and the two stage heating model are shown in Model II/C (Table 3, Figure $12B_1$, $12B_2$, $12B_3$). Note that the calculated maturation value in the northern San Juan Basin (R_o=1.39) is approaching the observed maturation value (R_o=1.1-1.2), however a major difference still exists between the calculated and observed maturation values for the central Basin.

A greater level of coal maturation for the Fruitland Formation coals would be calculated if a geologic history was used in which the coals were buried at greater depths for longer time periods than in the above histories.

Maturation values obtained using one such geologic history along with the steady-state temperatures of the best-fit isothermal step model (Figure 6) are presented in Model I/B (Table 3, Figure 12C). For this model the calculated and observed maturation values agree for the north-central San Juan Basin (25 km south of the step edge) although the calculated maturation values are higher than observed values in the northern and southern Basin.

DISCUSSION

It was noted above that the steady-state isothermal step model shown in Figure 6 gives the best fit to the observed San Juan region heat flow. However, in general the coal maturation levels calculated from the steady-state temperature model and the generalized San Juan Basin geologic history (Figure 12A) do not agree with the observed levels of Fruitland Formation coal maturation in the central and northern San Juan Basin (Table 3). Only in the southern San Juan Basin, which is relatively unaffected by elevated temperatures in the San Juan Mountains and northern San Juan Basin, is the steady-state thermal model and generalized geologic history compatible with the observed level of coal maturation. Therefore the northern and central Basin must have undergone further heating than is predicted by the steady-state thermal model and the generalized San Juan Basin geologic history. Additional heating could result from either greater burial depths of the Fruitland coals or from elevated thermal gradients caused by magmatic emplacement in the crust. The variation of coal maturation across the San Juan Basin suggests that the thermal history of the San Juan region could be a result of various geologic histories and temperature models for different regions in the Basin. The calculated and observed maturation levels may also indicate that additional factors have influenced the level of Fruitland coal maturation. The relation of

various thermal models to the coal maturation levels in the San Juan Basin are discussed below.

The Fruitland coals in the southern San Juan Basin have a relatively low level of maturation, indicating that the southern Basin has experienced little preferential heating since Late Cretaceous time. Present day heat-flow measurements in the region are consistent with this conclusion. The observed level of coal maturation in the southern Basin is predicted from a thermal model using a generalized San Juan Basin geologic history and a steady-state temperature model which leaves the heat flow unchanged since the Fruitland coal deposition (Model I/A; Table 3, Figure 12A). It would thus appear that the southern Basin has not been exposed to any major heating events since Late Cretaceous time. The results also suggest that the Fruitland coals of the southern San Juan Basin have not been buried deeper than about 1 km for any significant amount of time, because greater burial depths would cause higher maturation levels (Table 3, Figure 12A, $12B_3$, and 12C).

The Fruitland coals of the northern San Juan Basin, in contrast to the southern Basin coals, have a high level of maturation. The northern Basin is presently an area of high heat flow. These facts suggest major heating in the northern Basin. From the above results (Model I/A; Table 3, Figure 12A) it may be seen that the level of coal

maturation in the northern San Juan Basin cannot be obtained from the above generalized San Juan Basin geologic history and the steady-state isothermal step temperature distribution model. The large scale Oligocene magmatic activity associated with the San Juan Mountains may have been a major source of heat for the northern San Juan Basin. The Laramide volcanic activity in the region may also have provided additional heat. The two-stage heating model presented above (Table 3) combines the thermal regime of the isothermal step model with two periods of more elevated temperatures (corresponding approximately to the Laramide and Oligocene periods of volcanism). When this temperature model is combined with a local northern San Juan Basin geologic history (Figure $12B_1$), the level of Fruitland coal maturation calculated for the northern Basin is approximately the observed maturation level (Model II/C, Table 3).

The southern extent of the shallow heat source is an important parameter for the two-stage heating model and its relation to the northern San Juan Basin coal maturation level. The best-fit steady-state isothermal step was found to extend southward to a position beneath the northern San Juan Basin (Figures 3 and 6). This location, being near the uplifted edge of the northern Basin, may be compatible with the regional geology. In the two stage heating model the southern extent of the shallow heat source was taken to be the same as for the best-fit isothermal step. This location

leads to rough agreement between calculated and observed Fruitland coal maturation levels in the northern Basin (Model II/C; Table 3, Figure $12B_1$). However there is little evidence for magmatic activity in the northern Basin on the scale that would be expected for such a shallow heat source (i.e. 1200 ^{o}C at 10 km depth). Perhaps a more reasonable place for the southern extent of the shallow heat source would be at the edge of the San Juan volcanic field batholith, north of the San Juan Basin and ~25 km north of the source edge used in the two stage heating model. If this more northerly location is taken as the extent of the shallow heat source, then it is unlikely that the magmatic activity in the San Juan Mountains would supply much heat to the northern San Juan Basin due to the diffusion of heat away from the source. Note that the calculated level of coal maturation decreases rapidly for locations beyond the source edge (Table 3).

It is also unlikely that the level of Fruitland coal maturation in the central San Juan Basin is due to shallow heat sources associated with magmatic activity in the San Juan Mountains. Again there is little evidence to suggest shallow magmatic activity within the Basin which could account for the required heating. In addition, if the shallow heat source were to extend as far south as necessary to produce the observed coal maturation level in the central Basin, the resulting maturation level in the northern Basin would be too great.

Observed levels of Fruitland coal maturation in the central and northern San Juan Basin could be obtained using the best-fit steady-state step model if burial depths deeper than those in the given San Juan Basin geologic history are allowed. It is theoretically possible to calculate the observed coal maturation levels in the Basin by varying the geologic history model across the Basin; however, the geologic models must be evaluated as to the reasonability of the required geologic histories. The two variables in this type of model are the depth of burial of the Fruitland coals and the time the coals remain at a given depth. The temperature distribution is assigned by the best-fit steady-state isothermal step model. Generally speaking, deep burial depths over a relatively short time period will have the same effect on the coal maturation as shallow burial depths over a long time period.

An example of a model for a relatively shallow burial depth and a long time period of heating has been previously presented (Model I/B; Table 3, Figure 12C). In this model maturation values are calculated by using a 2 km burial depth over about a 50 my time span coupled with the steady-state isothermal step temperature distribution. The resulting maturation level calculated for the Fruitland coals of the central San Juan Basin approximate the observed maturation level (Model I/B, Table 3). However, the calculated maturation levels for the northern and southern Basin coals are higher than the observed levels (Model I/B,

Table 3). The calculated coal maturation level for the northern Basin would better approximate the observed level if shallower burial depths were used in the model (e.g. burial depths on the order of 1.5 km). The southern Basin coal maturation level has already been discussed, close agreement between observed and calculated maturation levels being obtained using the generalized San Juan Basin geologic history (Model I/A; Table 3, Figure 12A, i.e. a maximum burial depth of 1.3 km).

Even though the above combination of geologic histories result in calculated maturation levels which agree with observed maturation levels across the San Juan Basin, the reasonability of the required geologic histories must also be considered. The geologic histories given above require burial depths for the Fruitland Formation coals which are up to 1.8 km and 1.3 km greater in the central and northern San Juan Basin than in the southern Basin. In addition the northern and central Basin history discussed above requires a continuous 1.5-2 km burial depth for the Fruitland coals for a 50 my time period, while in the southern Basin (50 km away) the burial depth of the Fruitland coals ranges between 0.2 and 1.3 km during the same time period. Such a difference in the burial depths of the coals between the northern, central and southern San Juan Basin is not consistent with what is presently known about the geology of the San Juan Basin (Baltz, 1967; Fassett and Hinds, 1971; Stone et al, 1983). A continuous 1.5-2 km burial depth for

the Fruitland coals of the northern and central Basin over a 50 my time period is also inconsistent with the geology of the San Juan Basin (Baltz, 1967; Fassett and Hinds, 1971; Stone et al, 1983).

Instead of relatively shallow burial depths for long time periods, the observed maturation levels of the Fruitland coals in the San Juan Basin could result from deeper burial depths of the coals for a short time period. For example, the maturation level of the Fruitland coals in the central Basin could result from a 4 km burial depth for approximately 0.5 my or from a 3 km burial depth for about 5 my. Alternatively, if the timing of the generalized San Juan Basin geologic history was applied to the central Basin, burial depths on the order of 1.5 km greater than the southern Basin coal burial depths for their 73 my history would be required. The deep burial depths and the variation in burial depths across the Basin required by these geologic models are also inconsistent with what is presently known about the geology of the San Juan Basin (Baltz, 1967; Fassett and Hinds, 1971; Stone et al, 1983).

If the burial depth required to account for the observed coal maturation levels in the San Juan Basin are inconsistent with the geologic history of the Basin, then other sources of heat which could affect the maturation levels are required. The thermal source associated with the San Juan Mountains would seem to be a likely heat source for

the Basin, although it has been shown above that heat conduction associated with a deep thermal source and batholithic emplacement is not sufficient to produce the observed coal maturation levels in the Basin. However it may be possible that heat advected by water has contributed to coal maturation in the Basin. The present regional ground-water flow in the northern San Juan Basin is generally from recharge areas in elevated regions along the Basin margin to discharge areas along the San Juan River (Stone et al, 1983). This pattern of ground-water flow in the northern Basin also seems to have existed in the early Tertiary (Fassett and Hinds, 1971; Baltz, 1967) and perhaps a flow pattern similar to the modern pattern has existed since the formation of the San Juan Mountains in Oligocene time. Water flowing into the San Juan Basin from the San Juan Mountains area may have been heated enough to elevate temperatures in the northern and central Basin as it flowed through the region.

The heat source for the water may be associated with the San Juan batholith. Additional heat could also be provided by water heated during deep circulation. The water temperatures which would be required to produce the observed maturation level of the Fruitland coals are related to the time needed for the maturation level to be obtained. For example, the observed coal maturation level in the northern Basin would be reached in 70 my at 110 ^{o}C or in 10,000 years at 240 ^{o}C; and the observed maturation level in the central

Basin would be be reached in 70 my at 106 ^{o}C or in 10,000 years at 234 ^{o}C. Water temperatures in this range are known to occur in hydrothermal systems associated with magmatic intrusions (White and Williams, 1975). Similar temperatures could be produced by water circulation to depths on the order of 2-4 kms in the San Juan region with its present observed heat flow. Although the water temperatures required to produce the observed coal maturation levels may be obtained, the problem of transferring the available heat into the northern and central San Juan Basin is a complex one which will depend on the relationship between hydrologic and geologic parameters. It seems possible however that heat advection has contributed significantly to the maturation of coals in the San Juan Basin.

The levels of coal maturation in the northern and central San Juan Basin may be associated with water heated by magmas of the San Juan volcanic field. This would require the transport of the heated water over a distance of 50-100 km. An additional heat source could be very deep ground-water circulation in the San Juan region. Deep water circulation could have important ramifications in the interpretation of regional heat-flow data and coal maturation data for the San Juan area. Figure 13 presents a generalized hydrogeologic cross section of the San Juan Basin from southwest to northeast. Water flows into the central Basin from the north along steeply dipping beds and from the south along more gently dipping beds. The deepest

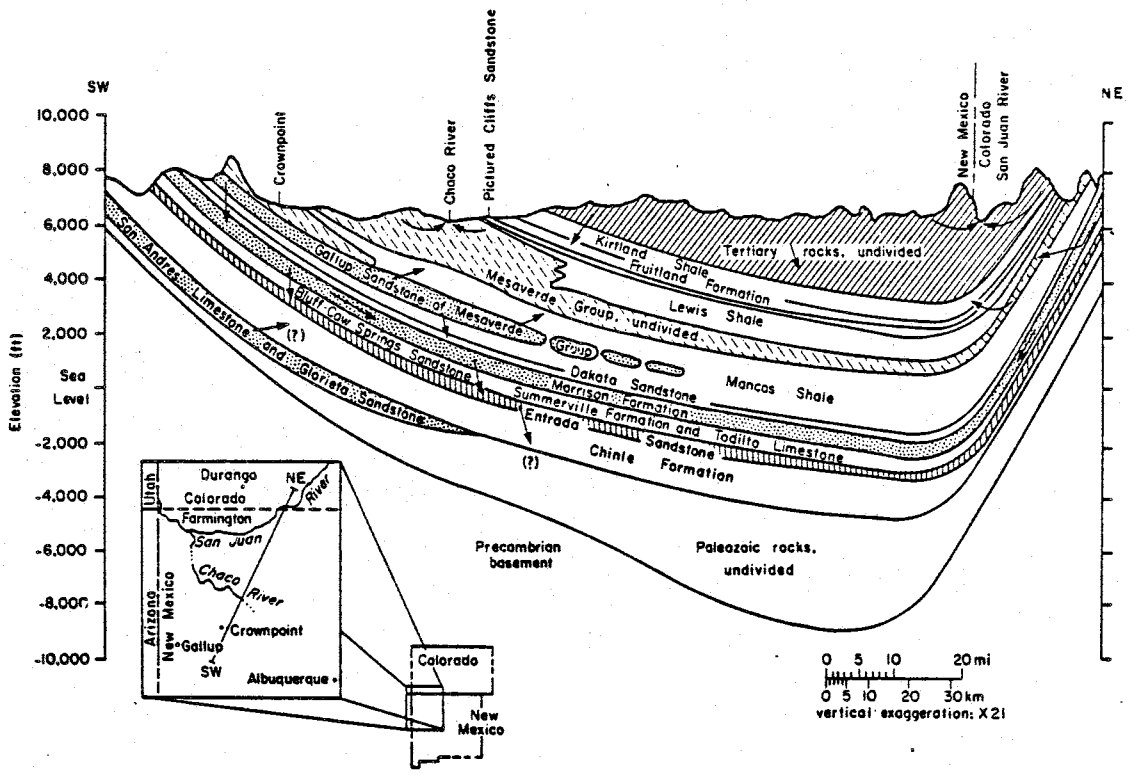

Figure 13. Hydrogeology of the San Juan Basin (Stone et al, 1983; reproduced with permission).

part of the aquifers in the San Juan Basin are approximately underneath the San Juan River, near the Colorado-New Mexico border. Water flowing into the Basin from the north could be warmed from heat associated with magmatic activity in the San Juan Mountains and from elevated temperatures at depth in the northern San Juan Basin. Water heated by a source in the San Juan Mountains and flowing into the Basin would warm the northern and central Basin. Warming of the northern and central Basin would be aided by leakage of heated water between aquifers and by the convective rise of water within aquifers. Similarly, deep ground-water circulation could also warm the Basin as water heated at depth moved upward between and within aquifers. Warming of the northern and central Basin by water heated in the San Juan Mountains and at depth in the San Juan Basin would imply a significant transfer of heat by advection and, consequently, that the observed surface heat flow is greater than the regional conductive flow. Thus if the San Juan Basin is being influenced by deep ground-water circulation, it may be possible to consider the true regional conductive flux only with very deep heat-flow measurements. Temperature gradients would need to be measured to depths of 3 km or more at some locations in the Basin. It has been suggested previously that shallow heat-flow measurements in the San Juan Basin (gradients measured to less than 0.75 km depth) are perturbed by ground-water movement (Reiter and Mansure, 1983). The above results suggest the possibility that deep

heat-flow measurements in the Basin may also be systematically influenced by deep ground-water circulation. The effects of the water movement could thus be an important factor in the consideration of the regional heat flow and level of coal maturation in the San Juan area.

Whatever heat sources are called upon to explain the level of coal maturation in the San Juan Basin; lower, more readily obtainable, temperatures are necessary as the time of heating increases. Longer times of maturation are consistent with the steady-state nature of the best-fit isothermal step model for the observed heat flow in the San Juan region. A steady-state model for the San Juan heat source requires that the heat source for the San Juan region has been replenished, perhaps as an overturning mantle plume, as a periodic input of magma into the region, and/or as a result of fundamental regional tectonic processes in the San Juan Basin, Colorado Plateau, and Southern Rocky Mountains.

CONCLUSIONS

A time-dependent isothermal step model of the San Juan region thermal regime shows that the observed heat flow in the region is best matched by a steady-state step isotherm. The best fit step extends from 30-98 km depth with the step edge located underneath the northern San Juan Basin. Long term heating in the San Juan region, i.e. Laramide, Oligocene, and perhaps younger heating events would not be inconsistent with the observed level of coal maturation in the central and northern San Juan Basin. Heating over a long time period requires lower temperatures to obtain the observed levels of coal maturation in the San Juan Basin. If the heat source in the San Juan region can be approximated as a steady-state heat source, then the source must be replenished.

The levels of coal maturation in the Fruitland Formation coals from the central and northern San Juan Basin require an influx of heat into the Basin in addition to the heat available from a steady-state isothermal step which has existed since the deposition of the coals. Additional heat could originate from such sources as shallow crustal magmatic activity, burial depth of the Fruitland coals greater than previously thought, or advection of heat by water movement. Some coal maturation in the northern Basin may be due to heat associated with magmatic activity in the

San Juan Mountains. However, it appears unlikely that most of the required heat is directly associated with the conduction of heat away from the San Juan batholith, because of the great distance between the batholith and the San Juan Basin. There is little evidence of magmatic activity in the Basin of the extent which would be required to produce the observed level of coal maturation in the central and northern Basin. It also appears that the burial depths required to produce the observed level of coal maturation are inconsistent with what is known about the geology of the San Juan Basin. It may be that heat advected by ground water movement has contributed significantly to the coal maturation in the central and northern Basin.

APPENDIX I: CALCULATION OF MODEL TEMPERATURES

Temperatures for the models given in the text were calculated using a finite difference approximation to solve a heat conduction problem with isothermal upper and lower bondaries and no flux side boundaries (see Figure 5, text). For a given temperature model the temperature varied with location, depth, and time in response to the geometry specified for the lower boundary. The model parameters were based upon values given by Chapman and Pollack (1977) and Schatz and Simmons (1972). In order to solve the conduction problem, values for density, specific heat, radiogenic heat production and thermal conductivity must be estimated.

The density model consisted of a two layer crust underlain by mantle (Figure 5, text). The upper crust was taken to extend from 0 to 8 km and to have an average composition of quartz diorite-granodiorite (Condie, 1976) with a density of 2.76 gcm^{-3} (Telford et al, 1978). The lower crust was taken to extend from 8 to 40 km depth and to have an average composition of diorite (Condie, 1976) with a density of 2.85 gcm^{-3} (Telford et al, 1978). The mantle compostion was taken to be that of a "hypothetical dunite", 90% fosterite and 10% fayalite (Schatz and Simmons, 1972), with a density of 3.38 gcm^{-3} (Telford et al, 1978).

The same layer thicknesses and compositions given above for the density model were used in the specific-heat model. Temperature dependent specific-heat values for minerals were taken from Robie et al (1978). The mineral composition for the rock types given above were taken from average values given in Hurlbut and Klein (1977).

Radiogenic heat production as a function of depth was based on the model of Chapman and Pollack (1977). Radiogenic heat production between 0 and 8 km depth was taken to supply 40% of the surface heat flow while the heat production between 8 and 40 km was taken as 0.25 $10^{-6}Wm^{-3}$, the heat production between 40 and 120 km depth was taken as 0.01 $10^{-6}Wm^{-3}$, and the heat production from below 120 km depth was taken as 0.084 $10^{-6}Wm^{-3}$. In the temperature models given in the text the surface radiogenic heat production (0-8 km) was based on the average heat flow in the southern San Juan Basin (67 mWm^{-2}), which was assumed to be the regional background heat flow, unaffected by magmatic activity and associated heat in the San Juan volcanic field. The heat production value thus assumed was consistent with the limited heat production data in the region (Reiter and Mansure, 1983). The average of four radiogenic heat production values in the region is 2.6 +/- 0.9 $10^{-6}Wm^{-3}$ (Reiter and Mansure, 1983) and the heat production model assumes a radiogenic heat production of 3.35 $10^{-6}Wm^{-3}$ in the layer from 0 to 8 km depth.

The thermal conductivity as a function of depth was based on the model of Schatz and Simmons (1972) and Chapman and Pollack (1977). However, the upper crustal thermal conductivity from 0 to 3 km depth was taken to be 2.0 $W(m^{o}K)^{-1}$; this value, which differs somewhat from the Chapman and Pollack (1977) model, was based upon conductivity and temperature data in the region (Reiter and Mansure, 1983; Reiter, unpub. data). The crustal thermal conductivity from 3 to 40 km depth was taken to be 2.5 $W(m^{o}K)^{-1}$ (Chapman and Pollack, 1977; Schatz and Simmons 1972). The thermal conductivity in the mantle was assumed to be temperature dependent (Schatz and Simmons, 1972). The mantle conductivity value was calculated as

$$K=2.5\ W(m^{o}K)^{-1} \qquad T<500\ ^{o}K$$

$$K=K_r + \max(K_L, K_{Lm}) \qquad T>500\ ^{o}K$$

where

$$K_r=0.55 * (T(^{o}K) - 500.0)$$

$$K_L=10^{-5}/(31.0 + 0.21 * (T(^{o}K))$$

$$K_{Lm}=300.0 * (1.0 + 0.001 * \text{depth (km)})$$

Using the above parameters and models the heat equation was solved for the two-dimensional, time-dependent case using numerical methods. In two dimensions the heat equation may be written as

$$(\hat{i}\,\partial/\partial x + \hat{k}\,\partial/\partial z) * K(T) * (\hat{i}\,\partial T(x,z,t)/\partial x + \hat{k}\,\partial T(x,z,t)/\partial z) + A(z) = \rho c(T)\,\partial T(x,z,t)/\partial t \qquad (1)$$

Note that K and c are implicitly functions of x, z, and t, as they are explicitly a function of T. The above derivatives were represented by their finite difference approximations and the change of temperature with time for a given model was calculated using the Crank-Nicholson method (Smith, 1978; Carnahan et al, 1969). The Crank-Nicholson method was chosen as it is relatively efficient and is stable for all time step sizes (Smith, 1978; Carnahan et al, 1969). For the Crank-Nicholson method equation 1 becomes

$$\begin{aligned}
&0.5\Big[(1/\triangle x^2)\big[K_{m+1/2,n,j+1}T_{m+1,n,j+1} + \\
&+ K_{m-1/2,n,j+1}T_{m-1,n,j+1} - \\
&- (K_{m+1/2,n,j+1} + K_{m-1/2,n,j+1})T_{m,n,j+1}\big] + (1/\triangle z^2) * \\
&*\big[K_{m,n+1/2,j+1}T_{m,n+1,j+1} + K_{m,n-1/2,j+1}T_{m,n-1,j+1}) - \\
&- (K_{m,n+1/2,j+1} + K_{m,n-1/2,j+1})T_{m,n,j+1}\big]\Big] + 0.5\Big[1/\triangle x^2 * \\
&*\big[K_{m+1/2,n,j}T_{m+1,n,j} + K_{m-1/2,n,j}T_{m-1,n,j} - \\
&- (K_{m+1/2,n,j} + K_{m-1/2,n,j})T_{m,n,j}\big] + (1/\triangle z^2) * \\
&*\big[K_{m,n+1/2,j}T_{m,n+1,j} + K_{m,n-1/2,j}T_{m,n-1,j}) - \\
&- (K_{m,n+1/2,j} + K_{m,n-1/2,j})T_{m,n,j}\big]\Big] + A = \\
&\qquad = (\rho c/\triangle t)\big[T_{m,n,j+1} - T_{m,n,j}\big]
\end{aligned} \qquad (2)$$

Where the grid around the point m,n at time step j is

	m-1	m	m+1
n-1	.	.	.
n	.	.	.
n+1	.	.	.

Equation 2 can be rearranged to solve for the temperature at time step j+1 given the temperature at time step j. In practice, due to the nonlinearities associated with the problem, the temperature solution was obtained by iterating the temperature calculation until it converged to a solution. For each time step the temperature solutions for the nodal points were considered to have converged when the sum of the nodal point temperatures differed from the sum of nodal point temperatures calculated 25 iterations earlier by less than a specified amount. The resulting nodal point temperatures typically varied less than 0.01 ^{o}C between iterations. The computer program used to make the temperature calculation is given at the end of the appendix.

The accuracy of the algorithm used for the temperature calculations was checked in a variety of ways:

(1) Simple examples were checked by hand,

(2) a solution for the problem T=T(z,t) with

$T(z)=0 \qquad t=0,\ 0<z<1$

$T(0)=0 \qquad t>0$

$T(1)=V \qquad t>0$

K=constant

A=0

was checked against results given by Carslaw and Jaeger (p. 313, 1959),

(3) a solution for the problem T=T(z,t) with

T(z)=0 t<0, 0<z<1

T(0)=T(1)=1.00 t>0

K=constant

A=0

was checked against results given by Carnahan et al (ex. 7.1, 1969),

(4) results compared favorably for a dike intrusion model of Horai (1974),

(5) a solution for the problem T=T(z,t) with

T(z)=0 t<0, 0<z<1

T(0)=T(1)=0 t>0

K=constant

$A=A_o$

was checked against results given by Carslaw and Jaeger (p. 130, 1959),

(6) results compare favorably with results given by Schatz and Simmons (1972) for a continental model with constant and with variable conductivity and heat production.

Attempting to balance accuracy and the computer time needed to obtain a solution, the distances between nodal points and the time increments used in the temperature calculations were varied according to the nature of the problem being solved. For models given in the text horizontal distances of 5 km and vertical distances of 2 km between nodal points were used. Variation of the distances between nodal points suggest that the precision of the temperature calculation was about +/-5% (or better) for this spacing. The time step size varied between 0.0625 and 2 my depending upon how rapidly the temperatures were changing within a given model. A 1 my time step was most frequently used. In most cases (except where the temperatures changed very rapidly) this time increment did not give significantly different results than smaller time steps.

The temperature model is rather insensitive to reasonable variations in the density (ρ), specific heat (c), radiogenic heat production (A), and thermal conductivity (K). Variations in the model density and specific heat will affect only transient temperature distributions and not the steady-state temperatures. The effect of density and specific heat will be most important for rapid variations of temperature with time. Table A1 presents variations in the calculated temperatures for different values of the quantity ρc. The temperatures shown in Table A1a are calculated for a model in which an isothermal step extending from 10 to 98 km depth is emplaced into a region initially having a uniform

surface heat flow of 67 mWm^{-2}. The temperatures presented are for 2 km depth at a location on the boundary of the model over the shallow portion of the isothermal step. The temperature variations shown are representative of the largest fluctuations of the near-surface temperatures with time encountered in the modelling. The near-surface temperature variations are of interest for the coal maturation calculations. Table Alb presents calculated temperatures for a model in which an isothermal step extending from 30 to 98 km depth is emplaced into a region initially having a uniform surface heat flow of 67 mWm^{-2}. The temperatures presented are also for 2 km depth at a location on the boundary of the model over the shallow portion of the isothermal step. Although significant temperature variations between the models do occur, they persist for only short times (Table Al). The range of the parameters presented in Table Al is surely extreme, and smaller variations in the model parameters would produce proportionally smaller differences between the calculated temperatures. The variation in the temperature model with density and specific heat appears to be insignificant except for short time periods of rapid temperature change.

Table A1. Variation of transient temperatures, T (in ^{o}C), for different values of ρc. Values of ρc are normalized with respect to the model values presented in text. Other model parameters are as presented in text.

a. Temperatures calculated for model in which an isothermal step extending from 10 to 98 km depth is emplaced into a region having a uniform initial surface heat flow of 67 mWm^{-2}.

	$\rho c/\rho c$ model				
	0.50	0.75	1.00	1.25	1.50
T(0.0 my)	66	66	66	66	66
T(0.5 my)	251	192	155	130	113
T(1.0 my)	288	271	246	221	196
T(1.5 my)	296	290	277	262	245
T(2.0 my)	297	295	290	280	269
T(2.5 my)	297	297	294	289	282
T(3.0 my)	297	297	296	294	289
T(steady state)	297	297	297	297	297

Table A1 (continued)

b. Temperatures calculated for model in which an isothermal step extending from 30 to 98 km depth is emplaced into a region having a uniform initial surface heat flow of 67 mWm^{-2}.

	$\rho c/\rho c$ model				
	0.50	0.75	1.00	1.25	1.50
T(0.0 my)	66	66	66	66	66
T(2.0 my)	78	71	69	68	67
T(4.0 my)	105	89	80	75	71
T(6.0 my)	120	107	96	87	81
T(8.0 my)	120	115	108	99	92
T(10.0 my	122	118	112	106	100
T(12.0 my	123	121	116	111	106
T(14.0 my)	123	121	119	115	110
T(16.0 my)	123	122	120	117	114
T(18.0 my)	123	123	121	119	116
T(20.0 my)	123	123	122	120	118
T(steady state)	123	123	123	123	123

Variations in the depth to the 1221 ^{o}C isotherm for different values of thermal conductivity in a region with a steady-state heat flow of 127 mWm^{-2} are shown in Table A2. Table A2a presents the depth variation for different values of the thermal conductivity in the near surface layer (0-3 km depth). Variations in the depth to the isotherm are small. Table A2b presents the depth variation for different thermal conductivity values throughout the entire depth range. The variation in the depth to the isotherm is more significant in this case. It should be noted however, that possible thermal conductivity values, at least in the near surface, are limited by observation (Reiter and Mansure, 1983). As such, the +/- 25% variation of the conductivity from the value given in the text may be the extreme limits on reasonable variations in the average near-surface thermal conductivity. If +/- 25% variation is also the extreme for conductivity values at depth, then the dependence of the temperature model on reasonable variations in thermal conductivity is relatively small (Table A2).

The temperature model is not significantly affected by the value of the radiogenic heat production. Table A3 presents the depth to the 1221 ^{o}C isotherm for different values of radiogenic heat production in a region with a steady-state heat flow of 127 mWm^{-2}. The variation in the depth for different heat-production values is small, indicating that the temperature model is not highly sensitive to variations in the radiogenic heat production.

From the above discussion it may be seen that the essence of the heat-flow anomaly across the San Juan Basin is produced by a temperature discontinuity and not by variations in radiogenic heat production or thermal conductivity across the region. The magnitude of the variation in the heat production and the thermal conductivity required to produce the observed heat-flow profile is unreasonably large. In addition there is no evidence for a systematic variation in heat production or thermal conductivity across the San Juan region (Reiter and Mansure, 1983).

Table A2. Depth to 1221 ^{o}C isotherm for different values of thermal conductivity, assuming a steady-state surface heat flow of 127 mWm^{-2}. Values of K are normalized with respect to the model values presented in text. Other model parameters are as in text.

---

a. Thermal conductivity varied only in the near-surface layer, 0-3 km depth.

K/K model	Depth to 1221 ^{o}C isotherm (km)
0.50	26
0.75	28
1.00	30
1.25	30
1.50	32

b. Thermal conductivity varied over the entire depth range.

K/K model	Depth to 1221 ^{o}C isotherm (km)
0.50	14
0.75	20
1.00	30
1.25	36
1.50	44

Table A3. Depth to 1221 ^{o}C isotherm for different values of radiogenic heat production assuming a steady-state heat flow of 127 mWm^{-2}. Values of A are normalized with respect to the model values presented in Figure 5. Other model parameters as in text.

A/A model	Depth to 1221 ^{o}C isotherm (km)
0.50	26
0.75	28
1.00	30
1.25	32
1.50	34

The computer program follows.

```
C THIS PROGRAM GIVES A FINITE DIFFERENCE SOLUTION TO THE
C 2-DIMENSIONAL TIME DEPENDENT HEAT FLOW (DIFFUSION)
C EQUATION FOR A STEP MODEL BOTTOM ISOTHERM, THE SURFACE
C BEING A ZERO DEGREE ISOTHERM AND THERE BEING NO FLUX OUT
C THE SIDE BOUNDARIES.  THE SOLUTION CONSIDERS CONDUCTIVITY
C AS A FUNTION OF POSITION AND TEMPERATURE AND RADIOACTIVE
C HEAT PRODUCTION AS A FUNCTION OF DEPTH.  THE CONDUCTIVE
C AND HEAT PRODUCTION VALUES USED ARE FROM CHAPMAN AND
C POLLACK (1977).  (SEE TEXT FOR EXPLANATION OF THIS MODEL
C AND THE VALUES USED.)  THIS MODEL ASSUMES A TWO LAYER
C CRUST OVERLYING MANTLE FOR THE DENSITY AND SPECIFIC HEAT
C MODELS.  THE UPPER CRUST IS TAKEN TO BE QUARTZ
C DIORITE-GRANODIORITE WITH AN AVERAGE DENSITY OF 2.76 G/CM3
C (TELFORD ET AL, 1978) AND A TEMPERATURE DEPENDENT SPECIFIC
C HEAT CALCULATED FROM A LINEAR COMBINATION OF THE MINERALS
C COMPOSING AN AVERAGE ROCK OF THIS COMPOSITION, THE
C COMPOSITION BEING BASED ON HURLBUT AND KLEIN (1977) AND
C THE TEMPERATURE DEPENDENCE OF THE MINERALS IS GIVEN BY
C ROBIE ET AL (1978).  THE LOWER CRUST IS TAKEN TO BE
C DIORITIC WITH AN AVERAGE DENSITY OF 2.85 G/CM3 (TELFORD ET
C AL, 1978) AND A COMPOSITION AND TEMPERATURE DEPENDENT
C SPECIFIC HEAT DETERMINED AS FOR THE UPPER CRUST.  THE
C MANTLE COMPOSITION IS TAKEN FROM SCHATZ AND SIMMONS
C (1972), WHO USE A HYPOTHETICAL DUNITE (Fo90Fa10) TO MODEL
C THE MANTLE.  THE DENSITY IS TAKEN AS 3.38 G/CM3 (TELFORD
C ET AL, 1978) AND THE SPECIFIC HEAT CALCULATED AS FOR THE
C CRUST.  SEE TEXT FOR MORE DETAILS.  NOTE THAT AT HIGHER
C TEMPERATURES SOME OF THE MINERALS IN THE ASSUMED CRUSTAL
C COMPOSITION ALTER THEIR STATE OR BREAK DOWN INTO OTHER
C MINERALS.  SOME OF THIS HAS BEEN CONSIDERED IN THE PROGRAM
C (CHANGE IN QUARTZ AT 844 K AND BREAKDOWN OF HORNBLENDE AT
C 1100 K) HOWEVER PROBLEMS IN THE RESULTS MAY BE ENCOUNTERED
C AT TEMPERATURES AROUND 1500 K AND HIGHER (I.E. THE RESULTS
C MAY BE INCORRECT.)  THE STEP ISOTHERM IS CONSIDERED TO BE
C EMPLACED INSTANEOUSLY AT A GIVEN TIME AND IS MAINTAINED
C THEREAFTER (NOTE DISCUSSION BY LACHENBRUCH ET AL, 1976).
C THE SOLUTION IS CALCULATED BY THE CRANK-NICHOLSON METHOD
C (SEE, FOR EXAMPLE, CARNAHAN ET AL, 1969).  NOTE IN USING
C THIS PROGRAM THAT LARGER TEMPERATURE CHANGES MAY REQUIRE
C SMALLER TIME STEPS IN ORDER TO OBTAIN GOOD RESULTS.

C T IS A MATRIX OF TEMPERATURES AND C THE CONDUCTIVITY
C MATRIX FOR THE MESH POINTS OF THE FINITE DIFFERENCE GRID.
C CPDUN IS THE MATRIX OF SPECIFIC HEATS FOR THE MESH POINTS,
C AND DENS AND DENC ARE ARRAYS CONTAINING THE DENSITY
C DISTRIBUTION.  TO, CO AND CPDUNO ARE MATRICES CONTAINING
C TEMPERATURE, CONDUCTIVITY AND SPECIFIC HEAT VALUES AT THE
C MESH POINTS FROM THE PREVIOUS TIME STEP.  NOTE THAT IN THE
C PROGRAM M IS A COLUMN NUMBER AND N A ROW NUMBER.  MATRIX
C COORDINATES ARE GIVEN AS A COLUMN AND THEN THE ROW, FOR
C EXAMPLE, T(1,2) REFERS TO THE TEMPERATURE AT THE MESH
C POINT LOCATED IN COLUMN 1 AND ROW 2.

      COMMON/T/T(151,101)/C/C(151,101)/CPD/CPDUN(151,101)
      COMMON/D/DENS(101)
```

```
      COMMON/CO/CO(151,101)/TO/TO(151,101)
      COMMON/CPDO/CPDUNO(151,101)/GRID/X,Y,DT,A1
      COMMON/PRMC/DX,AKD,KT/CDY/DY
      COMMON/PRMR/KK,TRY,KETCWR,H,V,TBOT
      common/GP/TIME,I,J,L,K
      COMMON/CPCF1/FWALB,FWAN,FWMIC,FWSAN,FWQTZ,FWTRM,FWDPS
      COMMON/FWENS
      COMMON/CPCF2/CFA,CFO

C SSTEP.DAT IS A DATA FILE FROM WHICH TEMPERATURE VALUES FOR
C ALL THE MESH POINTS MAY BE READ.  VALUES ARE OUTPUT TO
C WORK.OUT. PARAMETERS WHICH MAY BE CHANGED FREQUENTLY ARE
C READ FROM PARAM.DAT TO SAVE COMPILATION TIME WHEN RUNNING
C THE PROGRAM.

      OPEN(UNIT=1,DEVICE='DSK',ACCESS='SEQIN',FILE='SSTEP.DA
      OPEN(UNIT=21,DEVICE='DSK',ACCESS='SEQIN',FILE='PARAM.D
      OPEN(UNIT=20,DEVICE='DSK',ACCESS='SEQOUT',FILE='WORK.O

C H IS THE HORIZONTAL DISTANCE (KM) OF THE MODEL, INCLUDING
C THE POINTS OF THE FIRST AND LAST COLUMNS WHICH ARE USED AS
C MIRROR POINTS TO SATISFY THE NO FLUX BOUNDARY CONDITIONS.
C V IS THE DEPTH (KM) ASSOCIATED WITH THE MODEL FROM THE
C SURFACE TO THE LOWEST PORTION OF THE LOWER ISOTHERM.  I IS
C THE NUMBER OF COLUMNS OF MESH POINTS AND J IS THE NUMBER
C OF ROWS.  THE MESH POINT WHICH GIVES THE TOP CORNER OF THE
C STEP IS IN THE LTH COLUMN AND KTH ROW.  TBOT IS THE
C ASSIGNED CONSTANT LOWER BOUNDARY ISOTHERM.  DT IS THE TIME
C STEP USED (SEC). KTE IS THE NUMBER OF TIMES THE MODEL IS
C ADVANCED BY TIME STEP DT.  KKE IS THE MAXIMUM NUMBER OF
C TIMES THE TEMPERATURE CALCULATION IS ITERATED WITHIN EACH
C TIME STEP.  ICKVAL IS THE NUMBER OF ITERATIONS AFTER WHICH
C THE TEMPERATURE MATRIX IS CHECKED FOR CHANGE.  IF THE
C CHANGE IS LESS THAN TRYVAL THEN THE ITERATION FOR THAT
C PARTICULAR TIME STEP IS TERMINATED.  CALCULATED VALUES ARE
C OUTPUT TO WORK.OUT AFTER EVERY IWRT TIME STEPS AND FOR THE
C LAST TIME STEP.  IF THE VALUE OF KETCWR IS 1 THEN ALL
C VALUES (TIME, TEMPERATURE, CONDUCTIVITY, SPECIFIC HEAT,
C ETC.) ARE OUTPUT, OTHERWISE ONLY THE TIME, NUMBER OF
C ITERATIONS, DIFFERENCE BETWEEN LAST CHECKED MATRICES AND
C TEMPERATURES ARE OUTPUT.  ADTIME IS A TIME ADDED TO THE
C TIME CALCULATED WITHIN THE PROGRAM SO THAT THE PROPER TIME
C VALUE MAY BE OUTPUT WITH THE MODEL RESULTS; THIS WOULD BE
C NEEDED WHEN A MODEL IS RUN MORE THAN ONCE WITH THE PROGRAM
C AND THE FINAL OUTPUT OF ONE RUN IS USED AS THE INITIAL
C INPUT OF THE SUBSEQUENT RUN.  A1 IS THE RADIOGENIC HEAT
C PRODUCTION (IN CAL/(KM3*S) OF THE UPPER CRUST (0-8 KM) IN
C THE CHAPMAN AND POLLACK MODEL) WHICH IS RELATED TO THE
C SURFACE HEAT FLOW (A1=.4*Q0/8 KM IN THE CHAPMAN AND
C POLLACK MODEL).  VALUES ARE READ IN FROM PARAM.DAT AND
C ECHOED INTO WORK.OUT

      READ(21,*) H,V,I,J,L,K,TBOT,DT,KTE,KKE,ICKVAL,TRYVAL,
     $           IWRT,KETCWR,ADTIME,A1,kj
```

```
      WRITE(20,13) I,J
13    FORMAT(1X,'FULL MATRIX SIZE -IXJ- IS',I3,1X,'X',I3)
      WRITE(20,14) DT
14    FORMAT(1X,'TIME STEP SIZE=',E9.4,1X,'SEC')
      WRITE(20,15) KTE
15    FORMAT(1X,'NUMBER OF TIME STEPS PERFORMED IS ',I3)
      WRITE(20,16) ICKVAL
16    FORMAT(1X,'MATRIX CHECKED FOR CHANGE EVERY',I3,1X,
     $'ITERATIONS')
      WRITE(20,17) TRYVAL
17    FORMAT(1X,'ITERATION FOR A TIME STEP TERMINATED IF THE
     $CHANGE IN SUCCESSIVE CHECKED MATRICES IS LESS THAN',F6.3
      WRITE(20,18),H
18    FORMAT(1X,'THE HORIZONTAL DISTANCE (INCLUDING MIRROR
     $POINTS) IS ',F6.2)
      WRITE(20,19),V
19    FORMAT(1X,'THE DEPTH TO STEP BOTTOM IS ',F6.2)
      WRITE(20,20),TBOT
20    FORMAT(1X,'THE BOTTOM ISOTHERM TEMPERATURE IS ',F7.2)
      WRITE(20,21),L,K
21    FORMAT(1X,'COORDINATES OF L,K ARE ',2I6)
      WRITE(20,12) A1
12    FORMAT(1X,'SURFACE RAD. HEAT GENERATION IS',F9.4,2X,
     $'CAL/S*KM**3')

C CALCULATION OF HORIZONTAL GRID SPACING (DX) AND VERTICAL
C GRID SPACING (DY).  CALCULATION OF SOME NUMBERS USED
C FREQUENTLY THROUGHOUT THE PROGRAM.

      DX=H/(I-1)
      DY=V/(J-1)
      X=DX**2
      Y=DY**2
      KDIV=K-1
      JDIV=J-1
      DENO=2*(X+Y)

C OUTPUT TO WORK.OUT OF DEPTH TO STEP TOP AND GRID SIZE.

      AKD=KDIV*DY
      WRITE(20,22) AKD
22    FORMAT(1X,'DEPTH TO STEP TOP IS ',F8.2)
      WRITE(20,23) DX,DY
23    FORMAT(1X,'GRID SPACINGS ARE ',2F6.2)

C INITIAL DISTRIBUTION READ FROM SSTEP.DAT, WHICH IS AN IXJ
C MATRIX

      DO 2 N=1,J
      READ(1,1) (T(M,N),M=1,I)
1     FORMAT(61F8.2)
2     CONTINUE

C ESTABLISHMENT OF ELEVATED ISOTHERM
```

```
      DO 3 M=1,L
3     T(M,K)=TBOT

      DO 5 N=K+1,J-1
5     T(L,N)=TBOT


C CALCULATION OF SPECIFIC HEAT AND CONDUCTIVITY VALUES FOR
C THE INITIAL TEMPERATURE DISTRIBUTION AND ASSIGNMENT OF
C MESH POINT DENSITIES.  SPECIFIC HEAT VALUES AT A
C TEMPERATURE ARE CALCULATED FROM TEMPERATURE FORMULAS GIVEN
C IN ROBIE ET AL (1978); THESE VALUES ARE CALCULATED IN
C JOULES/MOLE*DEG K AND CONVERTED  TO CAL/G*DEG C.  CON IS
C A CONVERSION FACTOR.  DENS IS A DENSITY ARRAY WITH DENSITY
C IN G/KM**3.


      CON=4.184

      FWALB=262.225*CON
      FWAN=278.211*CON
      FWMIC=278.333*CON
      FWSAN=278.333*CON
      FWQTZ=60.085*CON
      FWTRM=812.374*CON
      FWDPS=216.553*CON
      FWENS=100.389*CON
      CFA=203.778*CON
      CFO=140.778*CON


      II=1


      DO 60 N=1,J

      Z=(N-1)*DY
      IF(N.GT.K) II=L

      DO 60 M=II,I

C CONVERSION OF TEMPERATURES TO DEGREES KELVIN.
 .bl
      TK=T(M,N)+273.15

C TEMPERATURES WHICH EXCEED 1500 K ARE NOT REALLY
C APPROPRIATE FOR THE SPECIFIC HEAT CALCULATIONS WHICH
C FOLLOW, IN ADDITION USE TEMPERATURES OF LARGE MAGNITUDE
C SUCH AS THIS USUALLY ARE THE RESULT OF JAEGER'S(1964)
C APPROXIMATION FOR THE LATENT HEAT OF COOLING, THEREFORE
C TEMPERATURES WHICH ARE ABOVE THE GIVEN VALUE ARE ADJUSTED
C FOR THE SPECIFIC HEAT AND CONDUCTIVITY CALCULATIONS.
```

```
      IF(TK.GT.1500.00) TK=1500.00

C CALCULATION OF CONDUCTIVITY VALUES


      if(z.gt.3.0) go to 33
      c(m,n)=478.01
      go to 50
33    continue

      IF(Z.GT.40.) GO TO 35
      C(M,N)=597.51
      GO TO 50
35    CONTINUE
      IF(TK.GT.500.) GO TO 40
      CR=0.0
      GO TO 45
40    CR=.55*(TK-500.)
45    CONTINUE
      CL=1.E5/(31.+.21*TK)
      CLM=300.*(1.+.001*Z)
      C(M,N)=CR+AMAX1(CL,CLM)
50    CONTINUE

C CALCULATION OF SPECIFIC HEAT VALUES BY SUBROUTINE SPH.
C SEE INTRODUCTION AND SUBROUTINE FOR COMMENTS

      MSPH=M
      NSPH=N
      CALL SPH(Z,TK,MSPH,NSPH)

60    CONTINUE

C ASSIGNMENT OF DENSITY VALUES, SEE INTRODUCTION FOR MODEL
C USED.

      DO 70 N=1,J

      Z=(N-1)*DY

      IF(Z.GT.8.) GO TO 61
      DENS(N)=2.76E15
      GO TO 65

61    CONTINUE

      IF(Z.GT.40.) GO TO 62
      DENS(N)=2.85E15
      GO TO 65

62    DENS(N)=3.38E15

65    CONTINUE

C FOR THE INITIAL DISTRIBUTION (PRIOR TO THE FIRST TIME STEP
```

```
C BUT AFTER THE ASSIGNMENT OF THE ELEVATED ISOTHERM) VALUES
C OF TEMPERATURE, CONDUCTIVITY AND SPECIFIC HEAT FOR THE
C 'PREVIOUS' TIME STEP (I.E. TO, CO AND CPDUNO) ARE THE SAME
C AS THOSE CALCULATED FOR THE INITIAL DISTRIBUTION
C IMMEDIATELY AFTER THE ESTABLISHMENT OF THE ELEVATED LOWER
C ISOTHERM.

      DO 70 M=1,I
      TO(M,N)=T(M,N)
      CO(M,N)=C(M,N)
      CPDUNO(M,N)=CPDUN(M,N)
70    CONTINUE


C OUTPUT OF THE INITIAL VALUES OF PARAMETERS, TEMPERATURES,
C AND, IF DESIRED, CONDUCTIVITY, SPECIFIC HEAT AND DENSITY
C TO WORK.OUT.

      TIME=ADTIME

      CALL VALOUT(kj)


C ITERATION LOOPS, A NEW TEMPERATURE DISTRIBUTION IS
C CALCULATED FOR EACH TIME STEP USING FINITE DIFFERENCE
C TECHNIQUES.  KTE TIME STEPS ARE DONE.  FOR EACH TIME STEP
C THE TEMPERATURE DISTRIBUTION IS ITERATED THE NUMBER OF
C TIMES SPECIFIED BY KKE OR THE ITERATION CAN BE TERMINATED
C WHEN THE LAST DISTRIBUTION CHANGES LESS THAN A SPECIFIED
C AMOUNT.

      DO 9999 KT=1,KTE


C TKEEP IS A VALUE USED LATER IN CALCULATING THE CHANGE IN
C THE MATRIX AFTER ITERATION AND NEEDS TO BE SET TO 0 HERE.

      TKEEP=0.0

      DO 7999 KK=1,KKE


C CALCULATION OF TEMPERATURES FOR THE MODEL.  THE MODEL
C REGION IS DIVIDED INTO SUBREGIONS AND AN INTERLACING
C METHOD FOR COLUMNS AND/OR ROWS IS USED TO CALCULATE THE
C TEMPERATURES IN A SUBREGION.  DO LOOP PARAMETERS ARE PASSED
C TO THE SUBROUTINE IN THE CALL PARAMETER LIST.  VALUES
C RELATED TO THE DO LOOP WHICH MOVES THE CALCULATIONS UP AND
C DOWN IN THE REGION (N IN THE SUBROUTINE) ARE GIVEN FIRST
```

```
C AND VALUES WHICH MOVE THE CALCULATIONS ACROSS (M IN THE
C SUBROUTINE) ARE GIVEN NEXT.  THESE VALUES SHOULD APPEAR IN
C THE ORDER THEY DO IN A "DO" STATEMENT--INITIAL VALUE,
C TERMINAL VALUE, INCREMENT.


C DEEP SUBREGION OF MODEL.  FIRST SET OF ALTERNATING COLUMNS.

c      CALL CALCT(K,J-1,1,L+1,I-1,2)
      CALL CALCT(2,k-1,1,2,1,2)

C DEEP SUBREGION.  SECOND SET OF ALTERNATING COLUMNS.

c      CALL CALCT(K,J-1,1,L+2,I-1,2)
      CALL CALCT(2,k-1,1,3,1,2)

C CALCULATION OF TEMPERATURES FOR THE SHALLOWER PORTION OF
C THE MODEL.  FOR THIS PORTION INTERLACING IS DONE BY ROWS,
C ONE SET BEGINNING WITH ROW K-1 AND THE OTHER SET BEGINNING
C WITH ROW K-2.  CALCULATION PROCEEDS FROM DEEPER TO
C SHALLOWER DEPTHS.

C FIRST SET OF ALTERNATING ROWS

c      CALL CALCT(K-1,2,-2,i-1,2,-1)
      CALL CALCT(2,j-1,2,1+1,i-1,1)

C SECOND SET OF ALTERNATING ROWS

c      CALL CALCT(K-2,2,-2,i-1,2,-1)
      CALL CALCT(3,j-1,2,1+1,i-1,1)

C TEMPERATURES AND CONDUCTIVITIES IN COLUMN I ARE NOW MADE
C EQUAL TO THE TEMPERATURES AND CONDUCTIVITIES IN COLUMN I-2
C AND SIMILARLY THE TEMPERATURES AND CONDUCTIVITIES OF
C COLUMN 1 ARE MADE EQUAL TO THOSE OF COLUMN 3; THAT IS TO
C SAY THAT THE FIRST AND LAST COLUMNS TO THE MATRICES ARE
C USED AS MIRROR POINTS IN ORDER TO OBTAIN ADIABATIC SIDE
C BOUNDARIES.

      DO 3999 N=2,J-1
      T(I,N)=T(I-2,N)
      C(I,N)=C(I-2,N)
3999  CONTINUE

      do 4001 n=2,k-1
      T(1,N)=T(3,N)
      C(1,N)=C(3,N)
4001  continue


C THE CALCULATED MATRIX IS CHECKED EVERY ICKVALTH ITERATION
```

```
C FOR CHANGE IN THE MATRIX.  THIS IS DONE BY SUMMING THE
C VALUES FOR ALL THE MESH POINTS AND COMPARING THIS NUMBER
C WITH THE PREVIOUS SUM (FROM ICKVAL ITERATIONS BEFORE).
C IF THE DIFFERENCE BETWEEN THE TWO VALUES IS LESS THAN A
C SPECIFIED AMOUNT THE ITERATIVE PROCESS IS STOPPED.  IF IT
C HAS BEEN LESS THAN ICKVAL  ITERATIONS SINCE THE CHECK WAS
C DONE THESE STEPS ARE BYPASSED.  TO CHANGE THE FREQUENCY OF
C CHECKS CHANGE THE THE VALUE OF ICKVAL (IN PARAM.DAT) WHICH
C APPEARS AS THE SECOND ARGUEMENT OF THE MOD FUNCTION TO THE
C DESIRED NUMBER OF ITERATIONS AFTER WHICH THE CHECK IS TO
C BE DONE.  NOTE THAT THE MOD FUNCTION GIVES THE REMAINDER
C OF THE DIVISION OF THE NUMBER OF ITERATIONS BY THIS SECOND
C ASSIGNED NUMBER.


C CHECK IF ITERATION IS THE 25TH.

      CHK=MOD(KK,ICKVAL)
      IF(CHK.NE.0.0) GO TO 7900


C SUMMATION OF TEMPERATURE VALUES AT ALL POINTS (CALLED
C TSAVE) AND CALCULATION OF THE DIFFERENCE (CALLED TRY)
C BETWEEN THIS AND THE PREVIOUS SUM VALUE (WHICH HAS BEEN
C STORED IN TKEEP).


      TSAVE=0.0
      DO 7800 M=1,I
      DO 7800 N=2,J
7800  TSAVE=TSAVE+T(M,N)
      TRY=ABS(TSAVE-TKEEP)


C CHECK OF DIFFERENCE AGAINST THE SPECIFIED TOLERANCE.  IF
C THE DIFFERENCE IS LESS THAN THE TOLERANCE THE PROGRAM IS
C TRANSFERRED OUT OF THE ITERATION LOOP FOR THIS TIME STEP,
C IF NOT THE SUM VALUE IS STORED IN TKEEP AND THE ITERATION
C PROCESS CONTINUES.

      IF(TRY.LE.TRYVAL) GO TO 8000
      TKEEP=TSAVE
7900  CONTINUE

7999  CONTINUE
8000  CONTINUE


C CALCULATION OF TIME (IN M.Y.) OF THIS TIME STEP

      TIME=DT*KT/3.16E13+ADTIME


C END OF ITERATION LOOP.  OUTPUT OF PARAMETERS AND SOLUTIONS
```

```
C TO FILE WORK.OUT.  PARAMETERS ARE OUTPUT AFTER EVERY IWRT
C TIME STEP ITERATIONS.  NOTE ALSO THAT INITIAL VALUES (I.E.
C BEFORE ANY CALCULATIONS ARE DONE) ARE ALSO OUTPUT BY THIS
C SECTION.


C CHECK IF ITERATION IS A MULTIPLE OF IWRT.

      WRT=MOD(KT,IWRT)
      IF(WRT.NE.0.0) GO TO 8400


C OUTPUT OF VALUES

      CALL VALOUT(kj)


8400  CONTINUE


C AFTER COMPLETION OF CALCULATIONS FOR AN INDIVIDUAL TIME
C STEP TO, CO AND CPDUNO ARE RESET TO THE FINAL VALUES
C DETERMINED FOR T, C AND CPDUN IN PREPARATION FOR THE NEXT
C TIME STEP.  VALUES ARE NOT RESET FOR THE LAST TIME STEP AS
C THEY ARE NOT NEEDED FOR FURTHER CALCULATIONS.


      IF(KT.EQ.KTE) GO TO 9999

C RESET OF VALUES FOR NEXT TIME STEP

      DO 9900 n=1,k
      DO 9900 M=1,1
      CO(M,N)=C(M,N)
      TO(M,N)=T(M,N)
      CPDUNO(M,N)=CPDUN(M,N)
9900  CONTINUE

      DO 9910 n=1,j
      DO 9910 M=1+1,I
      CO(M,N)=C(M,N)
      TO(M,N)=T(M,N)
      CPDUNO(M,N)=CPDUN(M,N)
9910  CONTINUE

9999  CONTINUE


C OUTPUT OF FINAL VALUES WHEN KTE (LAST TIME STEP) IN NOT A
C MULTIPLE OF IWRT; IF KTE IS A MULTIPLE OF IWRT THE VALUES
C ARE OUTPUT NATURALLY AT AN EARLIER TIME.

       kt=kte
c      IF(WRT.NE.0.0) CALL VALOUT
       call valout(j)
```

```
C END OF PROGRAM


      CLOSE(UNIT=1)
      CLOSE(UNIT=21)
      CLOSE(UNIT=20)
      STOP
      END

C*************************************************************

C SUBROUTINE FOR TEMPERATURE CALCULATIONS AND RECALCULATION
C OF CONDUCTIVITIES AND SPECIFIC HEATS.

      SUBROUTINE CALCT(KSUB,JSUB,JSTP,LSUB,ISUB,ISTP)
      COMMON/T/T(151,101)/C/C(151,101)/CPD/CPDUN(151,101)
      COMMON/D/DENS(101)/CO/CO(151,101)
      COMMON/TO/TO(151,101)/CPDO/CPDUNO(151,101)
      COMMON/DIS/DIST(151)/GRID/X,Y,DT,A1
      COMMON/CDY/DY
      common/GP/TIME,I,J,L,K
      COMMON/CPCF1/FWALB,FWAN,FWMIC,FWSAN,FWQTZ,FWTRM,FWDPS
      COMMON/FWENS
      COMMON/CPCF2/CFA,CFO

      DO 999 N=KSUB,JSUB,JSTP

C CALCULATION OF MESH POINT DEPTH

      Z=(N-1)*DY

C ASSIGNMENT OF DENSITY FOR GIVEN DEPTH (Z)

      DEN=DENS(N)


      DO 400 M=LSUB,ISUB,ISTP

C CALCULATION OF APPROXIMATE CONDUCTIVITIES AT POINTS HALF A
C GRID SPACING AWAY FROM THE POINT UNDER CONSIDERATION.  THE
C NEED FOR THESE VALUES ARISE DUE TO THE FINITE DIFFERENCE
C APPROXIMATION TO THE HEAT EQUATION WHICH INVOLVES THE
C FIRST DERIVATIVES OF CONDUCTIVITY.  HERE THE APPROXIMATION
C OF THE FIRST DERIVATIVE WOULD INVOLVE VALUES AT POINTS OF
C HALF SPACING, THESE ARE ESTIMATED AS FOLLOWS.

      CMPO=.5*(CO(M,N)+CO(M+1,N))
      CMMO=.5*(CO(M,N)+CO(M-1,N))
      CNPO=.5*(CO(M,N)+CO(M,N+1))
```

```
      CNMO=.5*(CO(M,N)+CO(M,N-1))
      CMP=.5*(C(M,N)+C(M+1,N))
      CMM=.5*(C(M,N)+C(M-1,N))
      CNP=.5*(C(M,N)+C(M,N+1))
      CNM=.5*(C(M,N)+C(M,N-1))

C DETERMINATION OF RADIOACTIVE HEAT GENERATION (DEPTH
C DEPENDENT) AT THE MESH POINT.  MODEL FOLLOWS THAT OF
C CHAPMAN AND POLLOCK (1977).  THE HEAT GENERATION IS
C EXPRESSED IN CAL/(SEC*KM**3).

      IF(Z.GT.8.)  GO  TO 110
      A=A1
      GO TO 200
110   CONTINUE
      IF(Z.GT.40.)  GO  TO 120
      A=59.751
      GO TO 200
120   CONTINUE
      IF(Z.GT.120.)  GO  TO 130
      A=2.3901
      GO TO 200
130   A=20.076
200   CONTINUE


C CALCULATION OF TEMPERATURE AT MESH POINT M,N.

       T(M,N)=1./(.5*((CMP+CMM)/X+(CNP+CNM)/Y)+
     $DEN*CPDUN(M,N)/DT)*(A+(DEN*CPDUNO(M,N)/DT
     $-.5*((CMPO+CMMO)/X+(CNPO+CNMO)/Y))*TO(M,N)+.5*
     $((CMP*T(M+1,N)+CMM*T(M-1,N)+CMPO*TO(M+1,N)+
     $CMMO*TO(M-1,N))/X+(CNP*T(M,N+1)+CNM*T(M,N-1)+
     $CNPO*TO(M,N+1)+CNMO*TO(M,N-1))/Y))

C RECALCULATION OF CONDUCTIVITY AND SPECIFIC HEAT FOR THE
C NEWLY CALCULATED MESH POINT TEMPERATURE.

C TEMPERATURE IN DEGREES KELVIN

      TK=T(M,N)+273.15

C ADJUSTMENT OF TEMPERATURE IF USE OF JAEGER'S (1964) LATENT
C HEAT APPROXIMATION IS USED FOR THIS MESH POINT.

      IF(TK.GT.1500.00) TK=1500.00

C CALCULATION OF NEW CONDUCTIVITY


      if(z.gt.3.0) go to 233
      c(m,n)=478.01
      go to 250
233   continue
```

```
      IF(Z.GT.40.) GO TO 235
      C(M,N)=597.51
      GO TO 250
235   CONTINUE
      IF(TK.GT.500.) GO TO 240
      CR=0.0
      GO TO 245
240   CR=.55*(TK-500.)
245   CONTINUE
      CL=1.E5/(31.+.21*TK)
      CLM=300.*(1.+.001*Z)
      C(M,N)=CR+AMAX1(CL,CLM)
250   CONTINUE

C CALCULATION OF NEW SPECIFIC HEAT, SEE INTRODUCTION AND
C SUBROUTINES FOR COMMENTS.

      MSPH=M
      NSPH=N
      CALL SPH(Z,TK,MSPH,NSPH)

400   CONTINUE
999   CONTINUE


      RETURN
      END

C*************************************************************


C SUBROUTINE FOR OUTPUT OF TEMPERATURE, CONDUCTIVITY,
C DENSITY, AND SPECIFIC HEAT.


      SUBROUTINE VALOUT(kjs)

      COMMON/T/T(151,101)/C/C(151,101)/CPD/CPDUN(151,101)
      COMMON/D/DENS(101)/PRMC/DX,AKD,KT/CDY/DY
      COMMON/PRMR/KK,TRY,KETCWR,H,V,TBOT
      common/gp/time,i,j,l,k


      WRITE(20,8080) KT
8080  FORMAT(1X,'NUMBER OF TIME STEPS IS ',I4)
      WRITE(20,8090) TIME
8090  FORMAT(1X,'TIME ELAPSED SINCE ELEVATED ISOTHERM
     $ESTABLISHED IS ',F8.2,' M.Y.')
      WRITE(20,8100) KK
8100  FORMAT(1X,'NUMBER OF ITERATIONS ARE ',I4)
      WRITE(20,8110) TRY
8110  FORMAT(1X,'DIFFERENCES IN LAST MATRICES ARE ',F10.5)
      WRITE(20,8175)
8175  FORMAT(1X,'MESH POINT TEMPERATURES')
```

```
      DO 8182 N=1,kjs
      WRITE(20,8180) (T(M,N),M=1,I)
8180  FORMAT(151F8.2)
8182  CONTINUE

C IF DESIRED (I.E. KETCWR=1) CONDUCTIVITY, DENSITY AND
C SPECIFIC HEAT VALUES ARE ALSO OUTPUT.

      IF(KETCWR.NE.1) GO TO 8300

      WRITE(20,8190)
8190  FORMAT(1X,'MESH POINT CONDUCTIVITIES')
      DO 8202 N=1,J
      WRITE(20,8200) (C(M,N),M=1,I)
8200  FORMAT(81F8.2)
8202  CONTINUE
      WRITE(20,8210)
8210  FORMAT(1X,'VERTICAL DENSITY DISTRIBUTION FOR MESH
     $POINTS')
      WRITE(20,8220) (DENS(N), N=1,J)
8220  FORMAT(101E8.2)
      WRITE(20,8230)
8230   FORMAT(1X,'MESH POINT SPECIFIC HEATS')
      DO 8242 N=1,J
      WRITE(20,8240) (CPDUN(M,N), M=1,I)
8240  FORMAT(61F6.4)
8242  CONTINUE
8300  CONTINUE


8750  CONTINUE
      RETURN
      END


C*************************************************************


C SUBROUTINE TO CALCULATE SPECIFIC HEAT
C FOR USE IN TEMPERATURE CALCULATIONS


      SUBROUTINE SPH(Z,TK,M,N)

C COMMON BLOCK FOR SPECIFIC HEAT VALUES (CPD) AND FORMULA
C WEIGHTS * CONVERSION FACTOR (CPCF1 AND CPCF2) WHICH ARE
C USED TO CALCULATE SPECIFIC HEAT IN CAL/(G*DEG C).

      COMMON/CPD/CPDUN(151,101)
      COMMON/CPCF1/FWALB,FWAN,FWMIC,FWSAN,FWQTZ,FWTRM,FWDPS,FWE
      COMMON/CPCF2/CFA,CFO

C TEMPERATURE FACTORS (IN DEG K) USED IN THE SPECIFIC HEAT
C FORMULAS.
```

```
      TK2=TK**2
      TKM2=TK**-2
      TKMH=TK**-.5

C CALCULATION OF SPECIFIC HEAT.  MODEL HAS CRUST TO 40 KM
C DEPTH WITH MANTLE BELOW.  CRUST IS TWO LAYER, DIVIDED AT
C 8 KM DEPTH.  SEE INTRODUCTION FOR MORE MODEL SPECIFICS.

      IF(Z.GT.40.) GO TO 100

C FORMULAS FOR CRUSTAL MINERALS SPECIFIC HEAT.  VALUES ARE
C CALCULATED IN J/(MOLE*DEG K) FROM ROBIE ET AL (1978) AND
C CONVERTED TO CAL/(G*DEG C) FOR USE IN THE PROGRAM.

      CPAB=5.8394E2-(9.2852E-2)*TK+(2.2722E-5)*TK2-
     $(6.4242E3)*TKMH+(1.6780E6)*TKM2
      CPAB=CPAB/FWALB
      CPAN=5.1683E2-(9.2492E-2)*TK+(4.1883E-5)*TK2-
     $(4.5885E3)*TKMH-(1.4085E6)*TKM2
      CPAN=CPAN/FWAN
      CPMIC=7.5955E2-(2.1711E-1)*TK+(6.4333E-5)*TK2-
     $(9.5268E3)*TKMH+(4.7642E6)*TKM2
      CPMIC=CPMIC/FWMIC
      CPSAN=6.9337E2-(1.7170E-1)*TK+(4.9188E-5)*TK2-
     $(8.3054E3)*TKMH+(3.4622E6)*TKM2
      CPSAN=CPSAN/FWSAN
      IF(TK.GT.844.) GO TO 10
      CPQTZ=4.4603E1+(3.7754E-2)*TK-(1.0018E6)*TKM2
      GO TO 15
10    CONTINUE
      CPQTZ=5.8928E1+(1.0031E-2)*TK
15    CONTINUE
      CPQTZ=CPQTZ/FWQTZ
      IF(TK.GT.1100.) GO TO 20
      CPTDE=6.1310E3-(4.1890)*TK+(1.7568E-3)*TK2-
     $(8.5656E4)*TKMH+(5.1385E7)*TKM2
      CPTDE=CPTDE/FWTRM
      GO TO 25
20    CONTINUE
      CPD=1.9182E2+(8.3079E-2)*TK-(2.1718E-5)*TK2-
     $(4.2795E6)*TKM2
      CPD=CPD/FWDPS
      CPE=2.0556E2-(1.2796E-2)*TK-(2.2977E3)*TKMH+
     $(1.1926E6)*TKM2
      CPE=CPE/FWENS
      CPTDE=2.*CPD/3.+CPE/3.
25    CONTINUE

C CALCULATION OF CRUSTAL SPECIFIC HEAT.

      IF(Z.GT.8.) GO TO 80
```

```
      CPDUN(M,N)=.4075*CPAB+.1775*CPAN+
     $.04*(CPMIC+CPSAN)+.235*CPQTZ+.1*CPTDE

      GO TO 90

80    CONTINUE

      CPDUN(M,N)=.59*CPAB+.25*CPAN+.02*(CPMIC+CPSAN+CPQTZ)+
     $.1*CPTDE

90    CONTINUE

      GO TO 200


100   CONTINUE

C FORMULAS FOR MANTLE MINERALS SPECIFIC HEAT.  VALUES ARE
C CALCULATED IN J/(MOLE*DEG K) FROM ROBIE ET AL (1978) AND
C CONVERTED TO CAL/(G*DEG C) FOR USE IN THE PROGRAM.

      CPFA=1.7276E2-(3.4055E-3)*TK+(2.2411E-5)*TK2-
     $(3.6299E6)*TKM2
      CPFA=CPFA/CFA
      CPFO=2.2798E2+(3.4139E-3)*TK-(1.7446E3)*TKMH-
     $(8.9397E5)*TKM2
      CPFO=CPFO/CFO

C CALCULATION OF MANTLE SPECIFIC HEAT.

       CPDUN(M,N)=.9*CPFO+.1*CPFA


200   CONTINUE

      RETURN
      END
```

APPENDIX II: COAL MATURATION

The maturation of organic material into coal is thought to be basically a first order chemical reaction, exponentially dependent on temperature and linearly dependent on time (Lopatin and Bostick, 1974; Waples, 1980). The level of coal maturation is often measured by characteristics of the coal such as calorific value, volatile matter content, or vitrinite reflectance (Dow, 1977). Although the variation of maturation with temperature and time of heating is thought to be relatively straightforward, the variations of the characteristics used to define the level of maturation are not uniform over the maturation scale (e.g., see Bostick, 1973; Heroux et al, 1979). Vitrinite reflectance is commonly used as an indication of the level of maturation as it can be used over a wide range of maturation levels and vitrinite is one of the most common constituents of coal (Dow, 1977).

Several methods have been formulated to calculate the level of hydrocarbon maturation obtained for a given temperature history (Bostick, 1973; Hood et al, 1975; Royden et al, 1980; Waples, 1980; and Middleton, 1982). These methods attempt to calculate (for a given temperature history) a value of a parameter characteristic of the maturation level, such as vitrinite reflectance. The time-temperature index (TTI) of maturation presented by

Waples (1980) was used to calculate maturation levels in this study. The above methods were applied to the Gulf Coast region of the southern United States as an independent test of the methods. Measured vitrinite reflectance values for the Gulf Coast were taken from Dow (1978) and the temperature history used was based on the Gulf Coast geologic history presented by Williamson (1959). The TTI method was chosen because the resulting calculated vitrinite reflectances were more consistent with observed vitrinite reflectance than were values calculated using the other methods.

The TTI index represents the level of hydrocarbon maturation as

$$TTI = \sum_{n} 2^{n} \Delta t_{n}$$

where t_n is the time (in million years) spent by a sediment in the nth 10 ^{o}C temperature interval. The TTI method thus gives a doubling of maturation with each 10 ^{o}C increase in temperature. Waples (1980) arbitrarily chose n=0 for the 100-110 ^{o}C temperature range with lower temperatures having negative n values and the higher temperatures having positive n values. Calculated TTI values have been correlated to vitrinite reflectance values by Waples (1980). The TTI method was altered slightly in this study to allow the calculated maturation value to vary continuously as a function of temperature and time. The level of maturation

was therefore calculated as

$$TTI=\int 2^{(T(^{o}C)-105)/10}\ dt$$

where t is the temperature in ^{o}C of the sediment at time t.

In the present study TTI values were calculated for various temperature models using the Romberg numerical integration technique (Hornbeck, 1975). In the Romberg integration technique the first estimate of an integral is given by the trapezoidal rule:

$$TTI_{1,k}=(\triangle x/2)*(f(a) + f(b) + 2\sum_{j=1}^{m} f(a + j\triangle x))$$

where

$$\triangle x=(b-a)/(2^{k-1})$$

and

$$m=2^{k-1} - 1.$$

Additional values for the integral are then extrapolated according to the relation

$$TTI_{m,k}=1/((4^{m-1} - 1)*(4^{m-1}TTI_{m-1,k+1} - TTI_{m-1,k})).$$

The Romberg estimates of the integral is given by the $TTI_{mmax,1}$ term (Hornbeck, 1975).

The program used for the maturation calculations is given at the end of this appendix. The time increment used in the numerical integration varied from 0.0625 to 1.0 my (depending on how the temperatures varied with time as described in Appendix I). The accuracy of the computer program was checked by hand calculation for simple functions and by comparison with examples given in Hornbeck (1975). For the more complicated temperature functions, repeated calculations using different time steps suggest a precision on the order of +/- 2% for the calculated maturation values.

The computer program follows.

```
C ROMBERG INTEGRATION (SEE HORNBECK, 1975; CHAPTER 8). USED
C FOR CALCULATION OF TTI VALUES (WAPLES, 1980) FROM
C TEMPERATURE MODELS.  TEMPERATURES INCLUDE THE TEMPERATURE
C COMPONENTS FROM THE ISOTHERMAL STEP MODELS AND THE
C APPROPRIATE SURFACE TEMPERATURE FOR THE CHOSEN GEOLOGIC
C HISTORY.  NOTE THAT THE INDEXING OF THE INTEGRATION
C VALUES DOES NOT CORRESPOND TO THE SUBSCRIPTING OF VALUES
C IN HORNBECK (1975) IN A SIMPLE FASHION.  THIS RESULTS
C THE MANNER IN WHICH VALUES ARE STORED IN THE TE MATRIX
C IN THE PROGRAM.  THE PROGRAM HAS BEEN CHECKED AGAINST
C EXAMPLES IN HORNBECK (1975) AND IS CORRECT.

C ********************************************************
C * NOTE THAT TO WORK CORRECTLY THE PROGRAM NEEDS        *
C * TEMPERATURES AT 2N+1 POINTS IN TIME, WHERE THE TIME  *
C * VALUES ARE EVENLY SPACED.                            *
C ********************************************************


      DIMENSION TMP(300), TE(300,300)


C FILES USED BY PROGRAM.  DATA ARE INPUT FROM RI.DAT,
C RESULTS OUTPUT TO RI.OUT.

      OPEN(UNIT=1,DEVICE='DSK',ACCESS='SEQIN',FILE='RI.DAT')
      OPEN(UNIT=21,DEVICE='DSK',ACCESS='SEQOUT',FILE='RI.OUT')


C INPUT OF DATA.  TIMI IS THE INITIAL TIME M.Y.B.P. AND TIMF
C IS THE FINAL TIME IN M.Y.B.P. FOR THE TIME INTERVAL BEING
C INTEGRATED.  I IS THE NUMBER OF TEMPERATURE VALUES GIVEN,
C EACH VALUE REPRESENTING THE TEMPERATURE AT A GIVEN TIME.
C TMP IS THE ARRAY OF MODEL TEMPERATURES.  EACH TEMPERATURE
C IN THE ARRAY CORRESPONDS TO A SPECIFIC POINT IN TIME.  THE
C INPUT TEMPERATURES ARE ECHOED INTO THE OUTPUT FILE.

      READ(1,*) TIMI,TIMF,I
      READ(1,*) (TMP(M), M=1,I)
      WRITE(21,600) (TMP(M), M=1,I)
600   FORMAT(1X,300F8.2)


C INTEGRATION OF TTI FORMULA


C DEFINITION OF TEMPERATURE FUNCTION OF TTI METHOD WHICH IS
C TO BE INTEGRATED OVER THE GIVEN TIME INTERVAL.

      DO 20 M=1,I
      TF=(TMP(M)-105.)/10.0
20    TMP(M)=2**TF
```

```
C VALUE DEFINED FOR MORE EFFICIENT USE LATER IN THE PROGRAM.

      I1=I-1

C SETTING OF K VALUE, WHERE K IS THE MAXIMUM NUMBER OF
C COLUMN AND ROWS IN THE TABLE OF VALUES FOR THE ROMBERG
C INTEGRATION (SEE HORNBECK, 1975, EQN. 8.43, P. 152).
C THE LAST EXTRAPOLATED VALUE POSSIBLE WILL BE T(K,K).

      DO 30 K=1,50
      IK=2**(K-1)+1
      IF(IK.EQ.I) GO TO 40
30    CONTINUE
40    CONTINUE


C CALCULATION OF VALUES FOR ROMBERG INTEGRATION

      DO 1000 KR=1,K


C CALCULATION OF TRAPEZOIDAL RULE VALUES, FIRST COLUMN OF
C TABLE OF VALUES FOR ROMBERG INTEGRATION (SEE HORNBECK,
C 1975, EQN. 8.41, P. 151-152).

      KRM=KR-1
      IF2=2**KRM
      IM=IF2-1
      DT=(TIMF-TIMI)/(2.*IF2)
      TEF=0.0

C FOR FIRST ELEMENT IN THE INTEGRATION THE FOLLOWING
C CALCULATIONS ARE UNNECESSARY AND ARE THUS THEY ARE
C SKIPPED.

      IF(KR.EQ.1) GO TO 200

      DO 100 KT=1,IM

      KTMP=(KT*I1/IF2)+1
100   TEF=TMP(KTMP)+TEF
200   TEF=TEF*2.

C TRAPEZOIDAL VALUE

      TE(KR,1)=DT*(TMP(1)+TMP(I)+TEF)

C FOR FIRST ELEMENT IN THE INTEGRATION THE FOLLOWING
C CALCULATIONS ARE UNNECESSARY AND ARE THUS THEY ARE
C SKIPPED.

      IF(KR.EQ.1) GO TO 500

C TEO IS USED TO STORE THE LAST EXTRAPOLATED VALUE OF THE
C INTEGRATION SO THAT THE CONVERGENCE TO THE VALUES TO THE
```

```
C SOLUTION MAY BE CHECKED.  THE VALUE OF TE GIVEN HERE WAS
C DETERMINED IN THE PREVIOUS K ITERATION.

      TEO=TE(KRM,KRM)

C CALCULATION OF EXTRAPOLATED VALUES FOR ROMBERG
C INTEGRATION.  THE ROMBERG SOLUTION FOR THIS ITERATION IS
C GIVEN BY THE DIAGNOL ELEMENT IN THE SOLUTION, THE LAST
C VALUE CALCULATED.


      DO 500 KC=2,KR
      KCM=KC-1
      IF4=4**KCM

      TE(KR,KC)=1.0/(IF4-1)*(IF4*TE(KR,KCM)-TE(KRM,KCM))

500   CONTINUE


C OUTPUT OF THE CALCULATED VALUES FOR THE INTEGRATION.

      WRITE(21,700) (TE(KR,KC), KC=1,KR)
700   FORMAT(1X,300F11.3)


C FOR FIRST ELEMENT IN THE INTEGRATION THE FOLLOWING
C CALCULATIONS ARE UNNECESSARY AND ARE THUS THEY ARE
C SKIPPED.

      IF(KR.EQ.1) GO TO 1000



C CHECK OF THE CONVERGENCE OF THE CALCULATED VALUES TO THE
C SOLUTION OF THE INTEGRAL.  VALUES ARE CONSIDERED TO HAVE
C CONVERGED TO THE SOLUTION WHEN THE DIFFERENCE BETWEEN THE
C FINAL EXTRAPOLATED VALUES FOR TWO CONSECUTIVE ITERATIONS
C IS LESS THAN THE VALUE GIVEN IN THE "IF" STATEMENT.  IF
C THE DIFFERENCE IS SUFFICIENTLY SMALL THE INTEGRATION IS
C TERMINATED.

      CHK=(TE(KR,KR)-TEO)/TEO
      CHK=ABS(CHK)
      IF(CHK.LT.0.0001) GO TO 1500


1000  CONTINUE
1500  CONTINUE
```

```
C END OF PROGRAM

      CLOSE(UNIT=1)
      CLOSE(UNIT=21)

      STOP
      END
```

REFERENCES

Baltz, E. H., 1967, Stratigraphy and regional tectonic implications of Upper Cretaceous and Tertiary rocks, east-central San Juan Basin, New Mexico: United States Geological Survey Professional Paper 552, 101 p.

Bird, P., 1979, Continental delamination and the Colorado Plateau: Journal of Geophysical Research, v. 84, p. 7561-7571.

Bodell, J. M., and D. S. Chapman, 1982, Heat flow in the north-central Colorado Plateau: Journal of Geophysical Research, v. 87, p. 2869-2884.

Bostick, N. H., 1973, Time as a factor in thermal metamorphism of phytoclasts (coaly particles): 7th Congres International de Stratigraphie et de Geologie Carbonifere, Krefeld, 1971, Compte Rendu, v. 2, p. 183-193.

Bridwell, R. J., 1976, Lithospheric thinning and the late Cenozoic thermal and tectonic regime of the northern Rio Grande rift: New Mexico Geological Society Guidebook 27, p. 283-292.

Carnahan, B., H. A. Luther, and J. O. Wilkes, 1969, Applied numerical methods: New York, John Wiley and Sons, Inc., 604 p.

Carslaw, H. S., and J. C. Jaeger, 1959, Conduction of heat in solids: New York, Oxford University Press, 510 p.

Chapin, C. E., 1979, Evolution of the Rio Grande rift: A summary, in R. E. Riecker, ed., Rio Grande rift: Tectonics and Magmatism: Washington, D. C., American Geophysical Union, p. 1-5.

Chapman, D. S., and H. N. Pollock, 1977, Regional geotherms and lithospheric thicknesses: Geology, v. 5, p. 265-268.

Clarkson, G. and M. Reiter, in press, Analysis of terrestrial heat-flow profile across the Rio Grande rift and Southern Rocky Mountains in northern New Mexico: New Mexico Geological Society Conference Guidebook 35.

Condie, K. C., 1976, Plate tectonics and crustal evolution: New York, Pergamon Press, Inc., 288 p.

Cordell, L., 1978, Regional geophysical setting of the Rio Grande rift: Geological Society of America Bulletin, v. 89, p. 1073-1090.

Decker, E. R., and F. Birch, 1974, Basic heat-flow data from Colorado, Minnesota, New Mexico, and Texas, in J. H. Sass and R. J. Munroe, compilers, Basic heat-flow data from the United States: United States Geological Survey Open File Report 74-9, p. 5.1-5.59.

Decker, E. R., and G. J. Bucher, 1979, Thermal gradients and heat-flow data in Colorado and Wyoming: A preliminary report: Los Alamos Scientific Laboratory, LA-7993-MS, p. 1-9.

Dickinson, R. G., E. B. Leopold, and R. Marvin, 1968, Late Cretaceous uplift and volcanism on the north flank of the San Juan Mountains, Colorado, in Cenozoic volcanism in the southern Rocky Mountains: Colorado School of Mines Quarterly, v. 63, p. 125-148.

Dow, W. G., 1978, Petroleum source beds on continental slopes and rises: The American Association of Petroleum Geologists Bulletin, v. 62, p. 1584-1606.

Dow, W. G., 1977, Kerogen studies and geological interpretations: Journal of Geochemical Exploration, v. 7, p. 79-99.

Eaton, G. P., R. L. Christainsen, H. M. Iyer, A. M. Pitt, D. R. Mabey, H. R. Blank, Jr., I. Zeitz, and M. E. Gettings, 1975, Magma beneath Yellowstone National Park: Science, v. 188, p. 787-796.

Edwards, C. L., M. Reiter, C. Shearer, and W. Young, 1978, Terrestrial heat flow and crustal radioactivity in northeastern New Mexico and southeastern Colorado: Geological Society of America Bulletin, v. 89, p. 1341-1350.

Fassett, J. E., and J. S. Hinds, 1971, Geology and fuel reserves of the Fruitland Formation and Kirtland Shale of the San Juan Basin, New Mexico and Colorado: United States Geological Survey Professional Paper 676, 76 p.

Galloway, M. J., 1980, Hydrogeologic and geothermal investigation of Pagosa Springs, Colorado: Colorado Geological Survey Special Publication 10, 95 p.

Heroux, Y., A. Chagnon, and R. Bertrand, 1979, Compilation and correlation of major thermal maturation indicators: The American Association of Petroleum Geologists Bulletin, v. 63, p. 2128-2144.

Hood, A., C. C. M. Gutjahr, and R. L. Heacock, 1975, Organic metamorphism and the generation of petroleum: The American Association of Petroleum Geologists Bulletin, v. 59, p. 986-996.

Horai, K., 1974, Heat-flow anomaly associated with dike intrusion, 1: Journal of Geophysical Reseach, v. 79, p. 1640-1646.

Hornbeck, R. W., 1975, Numerical methods: New York, Quantum Publishers Inc., 310 p.

Hurlbut, C. S., Jr., and C. Klein, 1977, Manual of mineralogy: New York, John Wiley and Sons, Inc., 532 p.

International Committee for Coal Petrology, 1963, International handbook of coal petrography: Paris, Centre National de la Recherche Scientifique, 1 vol., variously paged.

Iyer, H. M., 1979, Deep structure under Yellowstone National Park, U.S.A.: A continental "hotspot": Tectonophysics, v. 56, p. 165-197.

Jaeger, J. C., 1964, Thermal effects of intrusion: Reviews of Geophysics and Space Physics, v. 2, p. 443-466.

Kaula, W.M., 1970, Earth's gravity field: Relation to global tectonics: Science, v. 169, p. 982-984.

Keller, G. R., L. W. Braile, J. W. Schlue, 1979, Regional crustal structure of the Rio Grande rift from surface wave dispersion measurements in Riecker, R. E., ed., Rio Grande Rift: Tectonics and Magmatism: Washington, D. C., American Geophysical Union, p. 115-126.

Kelly, V. C., 1950, Regional structure of the San Juan Basin: New Mexico Geological Society Guidebook 1, p. 101-108.

Lachenbruch, A. H. and J. H. Sass, 1978, Models of an extending lithosphere and heat flow in the Basin and Range province: Geological Society of America Memoir 152, p. 209-250.

Lipman, P. W., B. R. Doe, C. E. Hedge, and T. A. Steven, 1978, Petrologic evolution of the San Juan volcanic field, southwestern Colorado: Pb and Sr isotope evidence: Geological Society of America Bulletin, v. 89, p. 59-82.

Lipman, P. W. and H. H. Mehnert, 1979, The Taos Plateau volcanic field, northern Rio Grande rift, New Mexico, in Riecker, R. E., ed., Rio Grande Rift: Tectonics and Magmatism: Washington, D. C., American Geophysical Union, p. 289-311.

Lopatin, H. V., and N. H. Bostick, 1974, The geologic factors in coal catagenesis: Illinois State Survey Reprint 1974Q, p. 1-16.

Lucchita, I., 1979, Late Cenozoic uplift of the southwestern Colorado Plateau and adjacent lower Colorado River region: Tectonophysics, v. 61, p. 63-95.

Mareschal, J., 1979, Mechanisms of uplift preceding rifting: Tectonophysics, v. 94, p. 51-66.

Middleton, M. F., 1982, Tectonic history from vitrinite reflectance: Geophysical Journal of the Royal Astronomical Society, v. 68, p. 121-132.

Molenaar, C. M., 1983, Major depositional cycles and regional correlations of Upper Cretaceous rocks, southern Colorado Plateau and adjacent areas, in M. W. Reynolds and E. D. Dolly, eds., Mesozoic paleogeography of west-central United States: Rocky Mountain Section, Society of Economic Paleontologists and Mineralogists, p. 201-224.

Morgan, W. J., 1972, Plate motions and deep mantle convection: Geological Society of America Memoir 132, p. 7-22.

Olsen, K. H., G. R. Keller, and J. N. Stewart, 1979, Crustal structure along the Rio Grande rift from seismic refraction profiles, in Riecker, R. E., ed., Rio Grande Rift: Tectonics and Magmatism: Washington, D. C., American Geophysical Union, p. 127-143.

Plouff, D., and L. C. Pakiser, 1972, Gravity study of the San Juan Mountains, Colorado: United States Geological Survey Professional Paper 800-B, p. B183-B190.

Prodehl, C. and L. C. Pakiser, Crustal structure of the southern Rocky Mountains from seismic measurements: Geological Society of America Bulletin, v. 91, p. 147-151.

Reiter, M. and G. Clarkson, 1983a, Geothermal studies in the San Juan Basin and the Four Corners area of the Colorado Plateau, II. Steady-state models of the thermal source of the San Juan volcanic field: Tectonophysics, v. 91, p. 253-269.

Reiter, M. and G. Clarkson, 1983b, Relationships between heat flow, paleotemperatures, coalification and petroleum maturation in the San Juan Basin, northwest New Mexico and southwest Colorado: Geothermics, v. 12, p. 323-339.

Reiter, M., C. L. Edwards, H. Hartman, and C. Weidman, 1975, Terrestrial heat flow along the Rio Grande rift, New Mexico and southern Colorado: Geological Society of America Bulletin, v. 86, p. 811-818.

Reiter, M. and A. J. Mansure, 1983, Geothermal studies in the San Juan Basin and the Four Corners area of the Colorado Plateau, I. Terrestrial heat-flow measurements: Tectonophysics, v. 91, p. 233-251.

Rice, D. D., 1983, Relation of natural gas compostion to thermal maturity and source rock type in San Juan Basin, northwestern New Mexico and southwestern Colorado: The American Association of Petroleum Geologists Bulletin, v. 67, p. 1199-1218.

Robie, R. A., B. S. Hemingway, and J. R. Fisher, 1978, Thermodynamic properties of minerals and related substances at 298.15 K and 1 bar (10 pascals) pressure and at higher temperatures: United States Geological Survey Bulletin 1452, 456 p.

Royden, L., J. G. Sclater, and R. P. Von Herzon, 1980, Continental margin subsidence and heat flow: Important parameters in formation of petroleum hydrocarbons: The American Association of Petroleum Geologists Bulletin, v. 59, p. 173-187.

Sass, J. H., A. H. Lachenbruch, R. J. Munroe, G. W. Greene, and T. H. Moses, Jr., 1971, Heat flow in the western United States: Journal of Geophysical Research, v. 76, p. 6376-6413.

Schatz, J. F., and G. Simmons, 1972, Thermal conductivity of earth materials at high temperatures: Journal of Geophysical Research, v. 77, p. 6966-6983.

Smith, G. D., 1978, Numerical solution of partial differential equations: Finite difference methods: New York, Oxford University Press, 304 p.

Steven, T. A., 1975, Mid-Tertiary volcanic field in the southern Rocky Mountains, in B. F. Curtis, ed., Cenozoic history of the southern Rocky Mountains: Geological Society of America Memoir 144, p. 74-94.

Stone, W. J., F. P. Lyford, P. F. Frenzel, N. H. Mizell, and E. Padgett, 1983, Hydrogeology and water resources of the San Juan Basin, New Mexico: Hydrologic Report 6, New Mexico Bureau of Mines and Mineral Resources, 70 p.

Telford, W. M., L. P. Geldart, R. E. Sheriff, and D. A. Keys, 1978, Applied geophysics: New York, Cambridge University Press, 860 p.

Turcotte, D. L., and S. H. Emerman, 1983, Mechanisms of active and passive rifting: Tectonophysics, v. 94, p. 39-50.

Turcotte, D. L., and G. Schubert, 1982, Geodynamics applications of continuum physics to geological problems: New York, John Wiley and Sons, Inc., 450 p.

Tweto, O., 1975, Laramide (Late Cretaceous-Early Tertiary) orogeny in the southern Rocky Mountains, in B. F. Curtis, ed., Cenozoic history of the southern Rocky Mountains: Geological Society of America Memoir 144, p. 1-44.

Waples, D. W., 1980, Time and temperature in petroleum formation: Application of Lopatin's method to petroleum exploration: The American Association of Petroleum Geologists Bulletin, v. 64, p. 916-926.

White, D. F., and D. L. Williams, eds., 1975, Assessment of Geothermal Resources of the United States-1975: Geological Survey Circular 726, 155 p.

Williamson, J. D. M., 1959, Gulf Coast Cenozoic history: Transactions-Gulf Coast Association of Geological Societies, v. 9, p. 15-29.

Wolfe, J. A., 1978, A paleobotanical interpretation of Tertiary climates in the northern hemisphere: American Scientist, v. 66, p. 694-703.

Wright, P. M., 1966, Geothermal gradients and regional heat flow in Utah: Ph. D. thesis, University of Utah, Salt Lake City, U.S.A.

This dissertation is accepted on behalf of the faculty of the Institute by the following committee:

Advisor

10 July, 1984
Date